RPP-18399, Rev. 0

Electrochemical Corrosion Studies, Core 308, Segments 14R1 and 14R2, Tank 241-AY-102

J. B. Duncan, ChemMet, Ltd. PC
G. A. Cooke, CH2M HILL
Richland, WA 99352
U.S. Department of Energy Contract DE-AC27-99RL14047

EDT/ECN: EDT 820213 UC:
Cost Center: 7S110 Charge Code:
B&R Code: Total Pages: 64

Key Words: Tank 241-AY-102, Sludge, Corrosion Potential

Abstract: This document reports the results of electrochemical corrosion tests on A515 Grade 60 carbon steel coupons exposed to tank 241-AY-102 sludge under conditions similar to those near the bottom of the tank. The tests were performed to evaluate the corrossive behavior of the waste in contact with sludge that does not meet the chemistry control limits of Administrative Control (AC) 5.15, Corrosion Mitigation Program.

Release Approval 10-30-03 Date

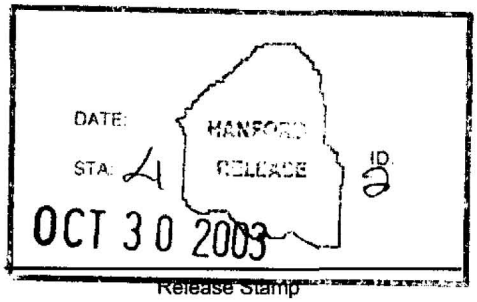

Release Stamp

Approved For Public Release

RPP-18399
Revision 0

Electrochemical Corrosion Studies, Core 308, segments 14R1 and 14R2, Tank 241-AY-102

J.B. Duncan
ChemMet, Ltd. PC

G.A. Cooke
CH2M HILL Hanford Group, Inc.

Date Published
October 2003

Prepared for the U.S. Department of Energy
Office of River Protection

Contract No. DE-AC27-99RL14047

TABLE OF CONTENTS

1.0 INTRODUCTION

The waste chemistry of the sludge in Tank 241-AY-102 does not meet Administrative Control (AC) 5.16, as stated in HNF-SD-WM-TSR-006, *Tank Farms Technical Safety Requirements*. Chemical additions have previously made to the supernatant in February 2001 (sodium hydroxide) and again in November 2001 (sodium nitrite). Tank 241-AY-102 has also been a receiver tank for periodic process condensate transfers from 241-AZ-151, dilute transfers from 241-C-106 as well as transfers from 244-AR Vault, TK-001. Corrosion potential of sludge samples taken in the April 2003 Tank 241-AY-102 sampling event have been evaluated in this document. This corrosion potential laboratory work is in support of the Tank 241-AY-102 Technical Safety Requirement (TSR) recovery plan, as directed in the Internal letter 03-TED-091/0302752, "Contract No. DE-AC27-99RL14047 - Recovery Plan to Restore Chemistry Control in Double-Shell Tank 241-AY-102," (letter 03-TED-091/0302752).

Because there are no near-term alternatives available to correct the sludge chemistry, an understanding of the corrosion behavior of the waste in the sludge region of the tank was required. However, the sludge resided deep within the tank where its oxygen content may be low enough to significantly retard corrosion mechanisms occurring at the tank wall.

The corrosion behavior of carbon steel samples, A515 Grade 60, immersed in Tank 241-AY-102 sludge was investigated by performing chronoamperometry at potentials close to the measured open circuit, E_{corr}, Tafel, and cyclic potentiodynamic polarization measurements. The test results provided information on whether or not the type of carbon steel used in constructing the tank is susceptible to either aggressive electrochemical corrosion or pitting mechanisms when exposed to sludge material under the conditions of storage in the tank. The corrosion potential testing was designed to reflect the conditions of storage near the tank bottom, as was practicable. In order to keep the sample in an anaerobic condition, the sludge was sampled by the core sample method. An extrusion platform was fabricated that allowed extrusion of the sludge in an anaerobic atmosphere using argon gas purge and monitored by an oxygen meter to ensure the absence of oxygen. This method was reported previously in RPP-12077, *Electrochemistry Corrosion Study for Tank 241-AY-102 Sludge*.

At a minimum, the sludge material was handled under an inert atmosphere at all times to preclude exposure to the oxygen in the atmosphere with the exception of the last two corrosion coupon runs. For the last two coupons, it was decided to mix the sludge in the ambient hot cell atmosphere then electrochemically interrogate the coupon. The sludge was then adjusted to bring the hydroxide content into the chemistry control specification by the addition of Tank 241-AY-102 supernatant. Another coupon was introduced to the sludge and electrochemically interrogated.

In order to minimize sample handling, a 500-mL sample jar used in the 222-S Laboratory 11 A hot cell area for routine extrusions was configured as the electrochemical cell. The design (reported previously in RPP-12077) was confirmed using the ASTM G5-94, *Standard Reference Test Method for Making Potentiostatic and Potentiodynamic Anodic Polarization Measurements*. The ASTM G5-94 was also used as a benchmark during testing to confirm instrument operation.

Tank 241-AY-102 core 308, segments 14R1 and 14R2 were individually extruded directly into dedicated electrochemical cells under anaerobic conditions. After extrusion, the electrochemical cells were continually subjected to a humidified argon gas stream. Tests performed on segment 14R2 were conducted as close to 60 °C as possible and comprised open circuit (E_{corr}), Tafel, and cyclic potentiodynamic scans as described in FH-0303055, 2003, *Test Plan/Procedure for Electrochemical Corrosion Testing of A515 Grade 60 Carbon Steel in 241-AY-102 Sludge.* The test coupons were purchased from Metal Samples, Mumford, AL and were prepared as per ASTM G5-94. The tank sludge was brought to temperature using a thermocouple in the sludge and an Omega Engineering Inc temperature controller.

Before being placed in the sludge, the coupon was removed from the inhibited paper, threaded onto the electrode shaft and cleaned as specified in the ASTM G5-94 and visually inspected for surface defects. The coupon was placed in the sludge and allowed to equilibrate for approximately eighteen hours before testing was initiated. The process was repeated for subsequent test coupons. Due to the sludge being heated and subsequent apparent volume reduction ("shrinking") which seemed to make less contact with successive test coupons, it was decided to maintain the second sample (segment 14R1) at ambient hot cell temperature (26 °C) for the next set of scans.

According to FH-030325, 2003, *Test Plan/Procedure for Electrochemical Corrosion Testing of A515 Grade 60 Carbon Steel in 241-AY-102 Sludge, Revision 1*, test coupons would be subjected to chronoamperometry, open circuit (E_{corr}), Tafel, and cyclic potentiodynamic scans.
The coupons were prepared and allowed to equilibrate as described above. For the last two coupons tested, the sludge was mixed in the hot cell ambient atmosphere using a tissue grinder before electrochemical testing began. The addition of 51 grams of Tank 241-AY-102 supernatant was added based upon the mass of segment 14R1 in the electrochemical cell, e-mail from K.G. Carothers to J.B. Duncan, "Supernatant Volume for Tank 241-AY-102 Corrosion Potential Testing" (Carothers 2003).

2.0 TESTING PROTOCOL

2.1 CORE 308 SEGMENTS 14R1 AND 14R2 EXTRUSION

Segments 14R1 and 14R2 were individually extruded under anaerobic conditions in 11 A1 hotcell. The configuration of the segment sampler and apparatus used was described in RPP-12077. A change in capping procedure from RPP-12077 as delineated in FH-0303055, Part-A, was followed.

Core 308, segment 14R1 riser 65 (LABCORE ID S03T001098) extruded approximately 18 inches of dark brown wet sludge. The whole segment was collected in one jar for electrochemical corrosion studies under anaerobic extrusion. The volume was estimated at 330 mL, and a total mass of 397.2 g. E-mail from A. L. Barnes to J. B. Duncan, "Tank 241-AY-102 C308" (Barnes 2003).

Core 308, segment 14R2 riser 65 (LABCORE ID S03T001099) extruded approximately 18.75 inches of dark brown, sludge slurry solids. The sample was collected for electrochemical corrosion studies under anaerobic extrusion. The volume was estimated at 340 mL, and a total mass of 407.9 g.

2.2 ELECTROCHEMICAL CORROSION TESTING

The samples were transported to 11 A3 hotcell and kept under continuous humidified argon purge (hereafter referred to as argon). The sample jars, which performed double duty as the electrochemical test cell, were positioned in tandem and connected together with tubing to receive the argon purge. Since FH-0303055 required that the sample be heated to approximately the tank sludge temperature (at that sampling level) of 60 °C, the farthermost sample jar from the argon source was configured with a heat belt (segment 14R2). This configuration allowed the working sample to be heated while the waiting sample received ambient temperature argon.

Once the first working sample (segment 14R2) attained the requisite temperature, a coupon composed of A515 Grade 60 steel was prepared according to ASTM G5-94 and visually inspected for noticeable surface defects. After preparation, the coupon was wrapped in several layers of Kimwipe[1] tissue, folded over the coupon assembly. [The coupon assembly consisted of a glass rod (insulator) covering a 316 SS threaded rod to receive the A515 Grade 60 coupon with Teflon® bullet spacer. The electrode lead end of the assembly consisted of a threaded section of the electrode shaft with a Teflon[2] washer, stainless steel washer, and stainless steel nut to tighten and hold the assembly together. The glass tube was fitted with a size 3 rubber stopper to affix the assembly into the electrochemical cell lid.]

The assembly was placed in tissue, being extremely careful not to touch the degreased coupon, and the tissue wrapped assembly was placed inside of a 50 mL centrifuge cone. The entire assembly in the centrifuge cone was then placed into 11 A hotcell using the bottle drop. The assembly was handled by securing the manipulator fingers to the cone and placing in the sled for transport to 11 A3 hotcell. The transfer time took approximately 5 minutes. Once in 11 A3, the assembly was removed using the manipulator fingers to secure the upper threaded portion (electrode lead connection end) and gently removing the centrifuge cone. The tissue was removed being careful not to touch the coupon. The coupon was then seated into the sludge through an opening in the center of the electrochemical cell lid. Visual observation is rather limited but when the white Teflon® bullet was no longer observed at the surface of the sludge, the coupon was considered placed and in contact with the sludge.

The coupon was allowed to equilibrate for eighteen hours before electrochemical scanning commenced. The scans were carried out in the order of E_{corr} (open circuit), Tafel, and cyclic polarization. The E_{corr} scan is used to determine if equilibrium has been established. The Tafel scan is used to calculate the electrochemical corrosion rate while the cyclic potentiodynamic scan is used to indicate pitting. All scans were against a Standard Calomel Electrode (SCE), the offset potential versus the Normal Hydrogen Electrode (NHE) is 0.242 V.

[1] KimWipe is a registered trademark of the Kimberly Clark Corp, Neeah, WI.
[2] TEFLON is a registered trademark of DuPont, Inc., Willmington, DE.

The Tafel scans were conducted from – 300 mV versus E_{corr} to + 300 mV versus E_{corr} at a scan rate of 0.166 mV/s. Under FH-0303055, cyclic scans were conducted from – 300 mV versus E_{corr} to 1,600 mV and back to – 300 mV versus E_{corr}. Under FH-3003325, the cyclic scans were conducted from – 300 mV versus E_{corr} to 1,000 mV and back to – 300 mV versus E_{corr}. These scans were much faster than the Tafel, as they were conducted around 5 mV/s.

Before and after the electrochemical scans on the Tank 241-AY-102 sludge were carried out, the operation of the instrument was confirmed using the ASTM G5-94 method. The scans are presented in Appendix A, Figures A-1 and A-2.

Under FH-303055 the A515 Grade 60 coupon designation is given in Table 2.1.

Table 2-1. A515 Grade 60 Test Coupon Identifier 14R2 Segment, High Temperature

Laboratory Book No.	Laboratory Book Coupon Identification	Viewed Under Scanning Electron Microscopy	LABCORE Identifier
HNF-N-2741	1A	Yes	S03T001559
HNF-N-2741	1B	Yes	S03T001560
HNF-N-2741	1C	No	NA
HNF-N-2741	1D	No	NA

Table 2-2. A515 Grade 60 Test Coupon Identifier 14R1 Segment, Room Temperature

Laboratory Book No.	Laboratory Book Coupon Identification	View ed Under Scanning Electron Microscopy	LABCORE Identifier
HNF-N-2741	2A	Yes	S03T001727
HNF-N-2741	3A	Yes	S03T001859
HNF-N-2741	3B	Yes	S03T001860
HNF-N-2741	1M	Yes	S03T001868
HNF-N-2741	2MOH	Yes	S03T001869

The scans associated with each of the above mentioned coupons are presented in Appendix A. The visual observation using a Scanning Electron Microscope are shown in Appendix B. Included in Appendix B are SEM scans of a control coupon surface. The control coupon was unwrapped from the inhibited paper that it was shipped in, visually inspected, and subjected to SEM interrogation. The control coupon SEM scans are presented as Figures B- 1 and B-2. It should be noted that the dark spots in Figure B-2 are specks of "dirt" and not corrosion products.

3.0 RESULTS

3.1 Segment 14R2 (60 °C) Scans

All coupons achieved an equilibrium during the E_{corr} versus time scans. The line was approaching an asymptote to a potential after approximately eighteen hours in the tank sludge. This measurement was taken during an open circuit, that is, there was no energy (current) input to the system, it was a closed system during this time.

However, once the Tafel scan began, current flowed into the cell and the open circuit would move from the E_{corr} versus time value to a different value. It must be remembered that E_{corr} is a measurement of the point where the reduction and oxidation vectors sum to zero. Any perturbation in a highly conductive environment (current input) may have the capacity to shift the E_{corr} point from one of equilibrium to a new position as a function of solution resistance, chemical speciation, and current input.

3.1.1 Coupon S03T001559

Coupon S03T001559 electrochemical scans are presented in Appendix A, Figures A-3 to A-6.

Coupon S03T001559 was the first coupon to be scanned in the high temperature sludge. The Tafel scan could not be used to calculate an electrochemical corrosion rate because the χ^2 goodness of fit calculation would not converge. The reason for this is not known but a possible hypothesis (as presented in Appendix C in the discussion of the χ^2 statistic) is that there are more than two principal redox reactions in the corroding system.

As indicated in the cyclic potentiodynamic scan, the return scan begins at lower current densities and then crosses the forward scan at approximately 700 mV. Once the return scan has crossed the forward scan the return scan remains at a higher current density. This scan is indicative of pitting due to the increase in current density, which in turn indicates an increase in surface area on the coupon. After the cyclic potentiodynamic scan, the coupon was removed and immediately placed in a vial of inhibited water. The coupon remained in the inhibited water until loaded out of the hot cell for the scanning electron microscope (SEM) evaluation (Appendix B). For all coupons loaded out of the hot cell to be viewed with the SEM, the handling was as described above.

Images of Coupon S03T001559 are shown in Appendix B, Figures B-12 through B-16. As noted in the narrative in Appendix B, this coupon showed several patches of corrosion up to several millimeters. Overall the pitting corrosion on this coupon was rather spectacular. The figures indicate pitting corrosion from shallow to more aggressive pitting that exposed individual metal grains (Figure B-16).

As with all coupons, there was a platinum to platinum scan run. This means that one platinum electrode was configured as the working electrode and the other platinum electrode was configured as the counter electrode. The logic was that platinum should not enter into a reaction with the tank sludge, but would be indicative of the appearance of new redox pairs, solution breakdown, etc.

3.1.2 Coupon S03T001560

Coupon S03T001560 electrochemical scans are presented in Appendix A, Figures A-7 to A-10.

Following Coupon S03T001559 was Coupon S03T001560, which was prepared as per ASTM G5-94 and placed in the heated sludge after Coupon S03T001559 was removed. The Tafel scan for Coupon S03T001560 was unable to be interrogated as to electrochemical corrosion rates. The χ^2 function would either return a value of greater than 400 for the GOF or it would not

converge to allow a calculation. For χ^2 greater than 100, the data is not following the Stern-Geary equation (Appendix C) and would be unreliable.

The cyclic polarization for Coupon S03T001560 did indicate a increase in current density during the return scan. The coupon was treated as described above for Coupon S03T001559 in preparation for SEM. The SEM is presented in Appendix B.

From the SEM photographs, Coupon S03T001560 showed not only pitting (Figure B-11) but also surface etching. This coupon was placed in approximately the same area as Coupon S03T001559 and did not exhibit as dramatic surface attack as did the first coupon to be exposed to the tank sludge.

3.1.3 Coupon 1C

Coupon 1C electrochemical scans are presented in Appendix A, Figures A-11 to A-14.

Coupon 1C did yield a Tafel scan that could be interrogated for an electrochemical corrosion rate. The results are presented in Table 3-3. The cyclic polarization did not indicate a pitting region. The coupon was not prepared for SEM due to the cyclic polarization scan response.

3.1.4 Coupon 1D

Coupon 1D electrochemical scans are presented in Appendix A, Figures A-15 to A-17.

Coupon 1D, the last high temperature run, likewise yielded a Tafel scan from which an electrochemical corrosion rate could be calculated. The cyclic polarization scan did not indicate a pitting regime and therefore the coupon was not prepared for SEM.

Table 3-3. A515 Grade 60 Corrosion Rates from Tank 241-AY-102 High Temperature Run

Coupon Identification	Temperature (°C)	E_{corr} (mV)	I_{corr} (μA)	B_c	B_a	Corrosion Rate (mpy)	X^2
S03T001559	54	--	--	--	--	--	--
S03T001560	54	--	--	--	--	--	--
1C	54	- 780	21.4	121	254	1.61	1.75
1D	54	-804	1.06	278	689	0.81	2.09

Note: When the sludge was disposed of in 11 A3 hotcell, visual observation noted "craters" where the working electrodes were placed. The same was noted for the Luggin bridge that housed the standard calomel reference electrode. The sludge appeared dry (albeit continually exposed to humidified argon flow) and indicated a "shrinking" away from the platinum counter electrodes. This indicates that the waste may be able to be used for only one or two scans at this temperature without impacting the area of surface-sludge contact.

3.2 Segment 14R1, Room Temperature Scans

Given the results from the above scans and the indication of pitting with Coupons S03T001559, S03T001560, and the observation of the "dried" sludge at the end of the run, it was decided to issue a revision to the test plan. The revised test plan (FH-0303325) called for a set of scans to be carried out at room temperature with the thought that the sludge would not dry out and attain a high resistance to current flow.

3.2.1 Coupon S03T001727

Coupon S03T001727 electrochemical scans are presented in Appendix A, Figures A-17.

Coupon S03T001727 was subjected to chronoamperometry at 100 mV versus E_{corr} for 18 hours. In this test, the potential (V) is fixed and the change in current (I) is measured. If there is pitting then an increase in current will be observed.

The resultant graph is presented in Appendix as Figure A-17. The graph appeared to yield electrochemical noise. There has been no correlation with tank sludge and chronoamperometric response to test coupons. However, the current did appear to increase therefore it was decided to prepare Coupon S03T001727 for load out and the SEM.

Figures B-7 indicates a single large patch of corrosion with obvious pitting occurring within the patch boundary.

3.2.2 Coupon S03T001859

Coupon S03T001859 electrochemical scans are presented in Appendix A, Figures A-18 to A-21.

Before Coupon S03T001859 was allowed to equilibrate and subjected to E_{corr}, Tafel, and cyclic polarization scans. The sample was stirred (under humidified argon gas flow) in the local vicinity of where the coupon would be placed. This was an attempt to bring in "fresh" sample material to interrogate. Electrochemical corrosion results are presented in Table 3-4. The cyclic scan did indicate an increase in current density. Therefore the coupon was prepared for load out and SEM interrogation.

Figures B-8 and B-9 exhibited surface effects that were barely visible as dark rough, patches (Figure B-8). There were three other areas that exhibited pitting as indicated in Figure B-9.

3.2.3 Coupon S03T001860

Coupon S03T001860 electrochemical scans are presented in Appendix A, Figures A-22 to A-25.

Coupon S03T001860 was allowed to equilibrate and subjected to E_{corr}, Tafel, and cyclic polarization scans. Electrochemical corrosion results are presented in Table 3-4. The cyclic scan

did indicate an increase in current density. Therefore the coupon was prepared for load out and the SEM.

The coupon exhibited on small patch of yellow-orange corrosion (visual examination). As shown in Figure B-5, indicated a corroded region characterized by a "deeping" effect of low areas between the striations.

3.3 Segment 14R1, Room Temperature Scans Mixed in Ambient Atmosphere and With Tank 241-AY-102 Supernatant

The humidified argon flow was stopped; the lid to the electrochemical cell was removed. Visual observation indicated craters in the sludge where the working electrode and the reference electrode had been placed. Although the sludge appeared to be moist and not dry, nonetheless it cannot be assured that total contact was made by the above-mentioned electrodes.

The sludge was homogenized using a tissue grinder. During the homogenization process an area near the jar wall and close to the bottom of the jar "felt" as if there was a drier section.

Electrochemical scans were performed on the homogenized in ambient atmosphere sample. After those scans were complete, approximately 51 grams of Tank 241-AY-102 supernatant was added per Carothers (2003) to ensure adequate hydroxide content. The sludge was mixed with the supernatant using the tissue grinder. Electrochemical scans were carried out on the hydroxide adjusted sludge.

After the electrochemical scans, the sample was centrifuged and submitted for per cent water, hydroxide concentration, and ion chromatography.

3.3.1 Coupon S03T001868

Coupon S03T001868 electrochemical scans are presented in Appendix A, Figures A-26 to A-30.

After the electrochemical scans, Coupon S03T001868 was placed in inhibited water and loaded out of the hot cell for SEM. The results of the Tafel electrochemical corrosion calculations are presented in Table 3-4. The coupon was prepared for load out and subsequent SEM evaluation.

The SEM interrogation of Coupon S03T001868 did not indicate evidence of corrosion (Figure B-3).

3.3.2 Coupon S03T001869

Coupon S03T001869 electrochemical scans are presented in Appendix A, Figures A-31 to A-34.

Coupon S03T001869 was placed in the sludge with the added Tank 241-AY-102 supernatant. Electrochemical scans were carried out and the coupon was prepared for load out for the SEM.

The SEM interrogation of Coupon S03T001869 did not indicate evidence of corrosion (Figure B-4).

Table 3-4 shows the electrochemical corrosion rates calculated from the respective Tafel scans using the POWERCORR[3] algorithm.

Table 3-4. A515 Grade 60 Corrosion Rates from Tank 241-AY-102 Room Temperature Run

Coupon Identification	Temperature (°C)	E_{corr} (mV)	i_{corr} (μA)	β_c	β_a	Corrosion Rate (mpy)	χ^2
S03T001727	26	--	--	--	--	--	--
S03T001859	26	-577	0.11	44.1	645	0.008	25.6
S03T001860	26	-672	3.38	40	334	0.25	0.78
S03T001868	26	-312	0.02	153	126	0.001	0.05
S03T001869	26	-289	0.44	315	671	0.033	5.51

4.0 DISCUSSION

Pitting corrosion was exhibited in Tank 241-AY-102 Core 308 segments 14R1 and 14R2. The evidence has been presented in both electrochemical cyclic polarization curves as well as scanning electron microscopic visual evidence. It should be noted that interrogating the same sample area multiple times, appears to induce a "lessening" response to the pitting corrosion mechanism. This localized effect was in most probability due to the effect described below by Thompson.

"The volume of the test solution should be large enough to avoid any appreciable change in its corrosiveness either through exhaustion of corrosive constituents or accumulation of corrosion products that might affect further corrosion," as discussed in *Handbook on Corrosion Testing and Evaluation* (Thompson).

Therefore, if the sludge chemistry around the working electrode is changed during testing, the resulting "new chemistry" can bias additional testing. This is due to the sample not being stirred coupled with the limited mass transport found in viscous samples.

It is possible that due to the chemical imbalance in the chemistry of the sludge, the analytical core analysis for segment showed a nitrate concentration of the interstitial fluid at 144 μg/mL, a nitrite concentration of less than detection limit (300 μg/mL), and a hydroxide concentration of 420 μg/mL (FH-0302530, 2003, *Tank 241-AY-102 FY 2003 Core Sample Analytical Results for the Final Report*) a regime for pitting corrosion has been established. According to SR17SP23, *Mechanism of Pitting Corrosion Prevention by Nitrite in Carbons Steel Exposed to Dilute Salt Solutions*, high nitrate concentrations allow the pitting potential to be close to the open circuit potential (E_{corr}). When nitrite was added to the solutions, the pitting potential moved several hundred millivolts (positive direction) away from the E_{corr}. Unfortunately, this was in a dilute

[3] POWERCORR is a registered trademark of AMETEK Advanced Measurement Technology, Inc., Oak Ridge, TN.

salt solution of pH 9.8 and nitrate concentrations were not as low as those reported in the analytical core segment above, let alone the more solid matrix of Tank 241-AY-102 sludge.

The authors cited in "Control of Stress Corrosion Cracking in Storage Tanks Containing Radioactive Waste" (Ondrejcin, Rideout, and Donovan); "Inhibition of Nuclear Waste Solutions Containing Multiple Aggressive Anions" (Congdon), and "Inhibiting Pitting Corrosion in Carbons Steel Exposed to Dilute Radioactive Waste Slurries" (Zapp and Hobbs) maintain that waste stored in carbon steel tanks, after having been made alkaline with substantial additions of sodium hydroxide carbon steel is essentially immune to uniform corrosion in this environment, but it is susceptible to localized corrosion in the forms of stress corrosion cracking and pitting, depending on the temperature and the specific waste chemistry. In addition to the nitrate ion, the waste may also contain chloride and sulfate that can induce localized corrosion. The initiation of localized corrosion in the carbon steel-waste environment can be prevented by nitrite in combination with a minimum pH or hydroxide concentration.

According to the relationship originally proposed by in *Pitting Corrosion of Metals* (Smialowska (1986) the pitting propensity can be characterized by a threshold electrochemical potential (E_p, pitting potential) which must be exceeded in the anodic direction for pitting to take place. The E_p is a function of the aggressive ion concentration and has the following functionality:

$$E_p = A - B*\log(C_x) \qquad (4\text{-}1)$$

Where:

A = experimentally determined electrochemical potential
B = 0.06 to 0. 2 V, experimentally determined
C = concentration of the aggressive ion.

Although not readily apparent from the above equation, there is a threshold concentration for the aggressive ion below, which there will be no pitting. A metal can be maintained in a state of immunity to pitting by control of the electrochemical potential and the concentration of the aggressive ion(s). With the sludge in Tank 241-AY-102, those aggressive ions have not been fully identified.

In ARH, *Complition of Hanford Corrosion Studies*, it was stated that pitting attack was more severe with carbon steel exposed to the simulated moist solid waste than to the simulated liquid waste. The pitting exhibited by the coupons immersed in the Tank 241-AY-102 sludge seemed to exhibit localized aggressive pitting modes.

As to which ions are the aggressive pit producing ions, the exact mechanism that occurs (past the theoretical models found in corrosion texts) cannot be determined at this time.

The conclusion must be that under the current chemistry, as tested, a pitting regime has been established. After the first few coupons in the same location, the pitting effect disappears; this is probably due to the exhaustion of the corrosive constituents (Thompson).

Therefore, without a further understanding of steel – surface film – chemical environment it is impossible to pinpoint specific ions, other than those relationships previously established for nitrate: nitrite: hydroxide concentrations.

5.0 CONCLUSIONS

The Tank 241-AY-102 sludge material continues to show electrochemical pitting behavior based on cyclic potentiodynamic scans. The pitting scan was observed on the high temperature tests and SEM evaluation confirmed the localized corrosion on the test coupon.

However, repeated scans using the same sludge material showed less significant evidence of electrochemical pitting. This could have been caused by localized depletion of aggressive components of the sludge, or by the sludge material drying and pulling away from the electrode at high temperature.

Test performed at lower temperature showed less electrochemical evidence of pitting but the SEM micrographs indicated evidence of attack on the coupon. When the sample was mixed with oxygen no increase in pitting was observed. Similarly, no pitting was observed when supernatant was added to bring the sludge into chemical balance.

Even though there are inconsistencies that cannot be fully explained (formation of new redox pairs, etc.), the Tank 241-AY-102 sludge has shown an electrochemical (verified by SEM) corrosion behavior that has not been observed in testing of other double shell tank waste sludge (Tank 241-AN-102 and Tank 241-AN-107). Tank 241-AY-102 may therefore merit further study.

6.0 RECOMMENDATIONS

From the study on Tank 241-AY-102 sludge, to make future studies meaningful, t he following is recommended:

- Homogenize the sample under anaerobic conditions before each electrochemical scan;
- Scan only one coupon per sample due to the effect mentioned above by Thompson, or
- Employ the use of a multi-potentiostat whereby four coupons may be scanned at one time independently of one another in one sample. This would allow statistics to be gained without a possible change in the sample from one scan to the next,
- Confirm the observation reported with fresh sample material obtained from the next tank 241-AY-102 core sample event. The current schedule for this sampling event is November 2003.
- Perform long-term corrosion testing in the tank or hot cell to evaluate the potential for pitting corrosion from Tank 241-AY-102 sludge.

7.0 REFERENCES

03-TED-091/0302752, 2003, "Contract No. DE-AC27-99RL14047 – Recovery Plan to Restore Chemistry Control in Double-Shell Tank 241-AY-102," (from R. J. Schepens to E. S. Aromi), Office of River Protection, Richland, Washington.

ARH-ST-111, 1975, *Compilation of Hanford Corrosion Studies*, Atlantic Richfield Hanford Company, Richland, Washington.

ASTM, 1999, *Standard Reference Test Method for Making Potentiostatic and Potentiodynamic Anodic Polarization Measurements*. Designation G5 – 94 (Reapproved 1999), American Society for Testing and Materials, West Conshohocken, Pennsylvania.

Barnes, A. L., 2003, "Tank 241-AY-102 C308," (email to J. B. Duncan, October 6), CH2M HILL Hanford Group Inc., Richland, Washington.

Carothers, K. G., 2003, "Supernatant Volume for AY-102 Corrosion Potential Testing," (e-mail to J. B. Duncan, October 9), CH2M HILL Hanford Group Inc., Richland, Washington.

CHG, 2002, "Chemistry Control Program," *Tank Farms Technical Safety Requirements*, Section 5.15, HNF-SD-WM-TSR-006, Revision 2-N, CH2M HILL Hanford Group, Inc., Richland, Washington.

Congdon, J. W., 1988, "Inhibition of Nuclear Waste Solutions Containing Multiple Aggressive Anions," *Materials Performance 15*, p. 34.

FH-0302530, 2003, *Tank 241-AY-102 FY 2003 Core Sample Analytical Results for the Final Report*, Fluor Hanford, Richland, Washington.

FH-0303055, 2003, *Test Plan/Procedure for Electrochemical Corrosion Testing of A515 Grade 60 Carbon Steel in 241-AY-102 Sludge*, Fluor Hanford, Richland, Washington.

FH-0303325, 2003, *Test Plan/Procedure for Electrochemical Corrosion Testing of A515 Grade 60 Carbon Steel in 241-AY-102 Sludge,* Revision 1, Fluor Hanford, Richland, Washington.

HNF-SD-WM-TSR-006, Revision 3, "Tank Farms Technical Safety Requirements," CH2M HILL Hanford Group, Inc., Richland, Washington.

Ondrejcin, R. S., S. P. Rideout, and J. A. Donovan, 1979, "Control of Stress Corrosion Cracking in Storage Tanks Containing Radioactive Waste," *Nuclear Technology 44,* p. 297.

RPP-12077, 2002, *Electrochemical Corrosion Study for Tank 241-AY-102,* Revision 0, CH2M HILL Hanford Group, Inc., Richland, Washington.

SR17SP23, 2002, *Mechanism of Pitting Corrosion Prevention by Nitrite in Carbon Steel Exposed to Dilute Salt Solutions*, Westinghouse Savannah River Company, Aiken, South Carolina.

Thompson, D. H., 1971, *Chapter 6, Handbook on Corrosion Testing and Evaluation,* W. H. Ailor (Ed.), John Wiley and Sons, Inc., New York, New York.

Zapp, P. E. and D. T. Hobbs, 1992, "Inhibiting Pitting Corrosion in Carbon Steel Exposed to Dilute Radioactive Waste Slurries," in *CORROSION/92*, paper no. 98, (Houston, Texas: NACE International).

APPENDIX A

ELECTROCHEMICAL SCANS

Figure A-1. ASTM Scan Before Tank 241-AY-102 Electrochemical Corrosion Testing

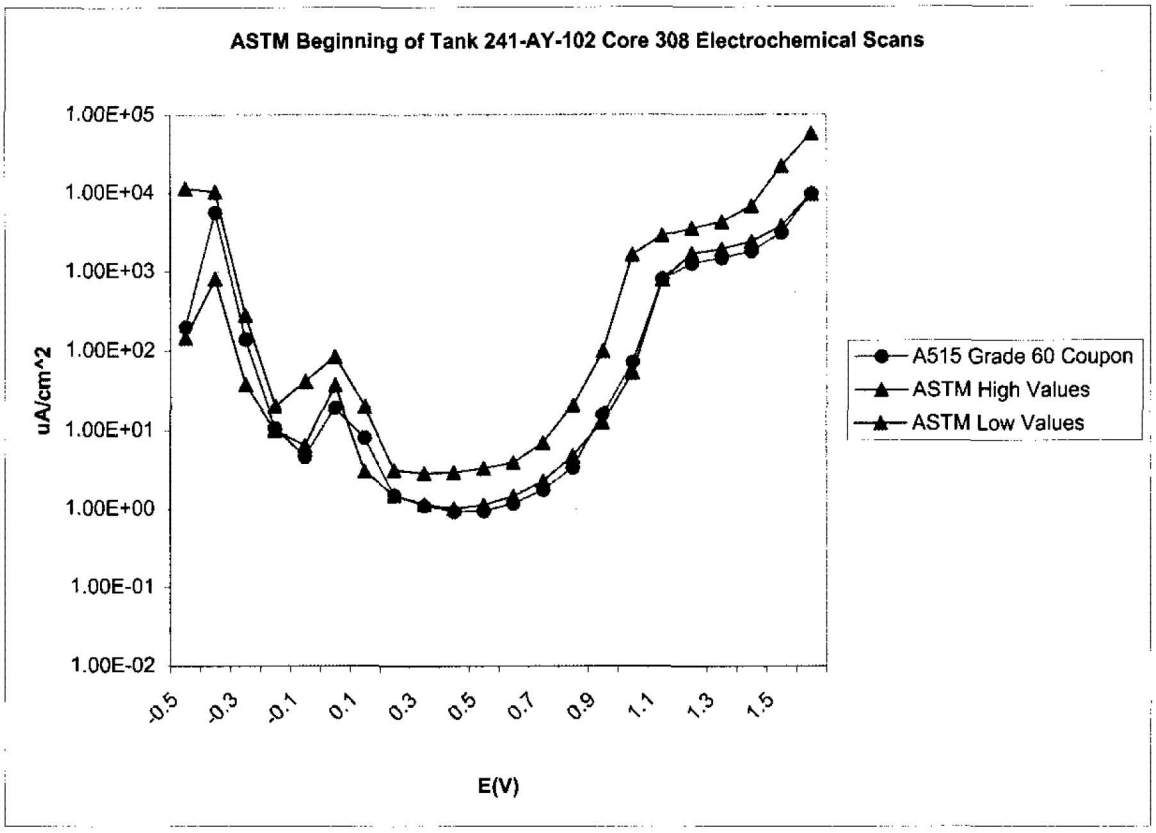

Figure A-2. ASTM Scan After Tank 241-AY-102 Electrochemical Corrosion Testing

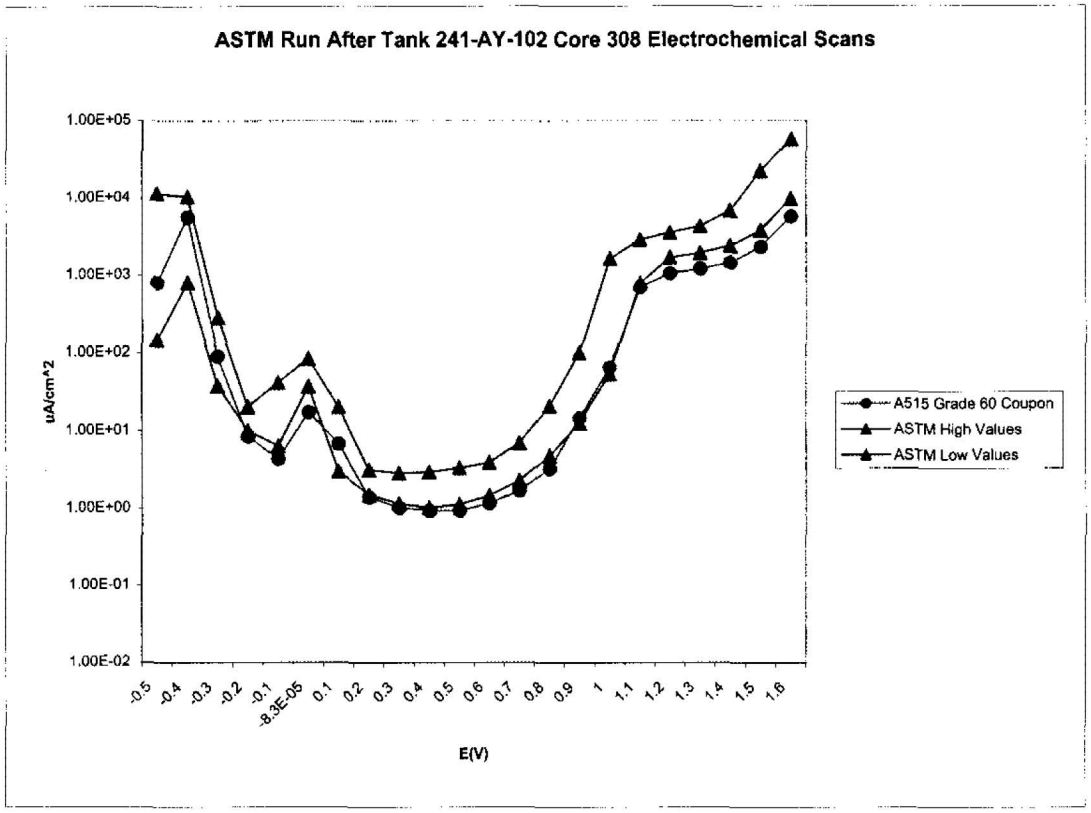

Figure A-3. S03T001559 E_{corr} versus Time

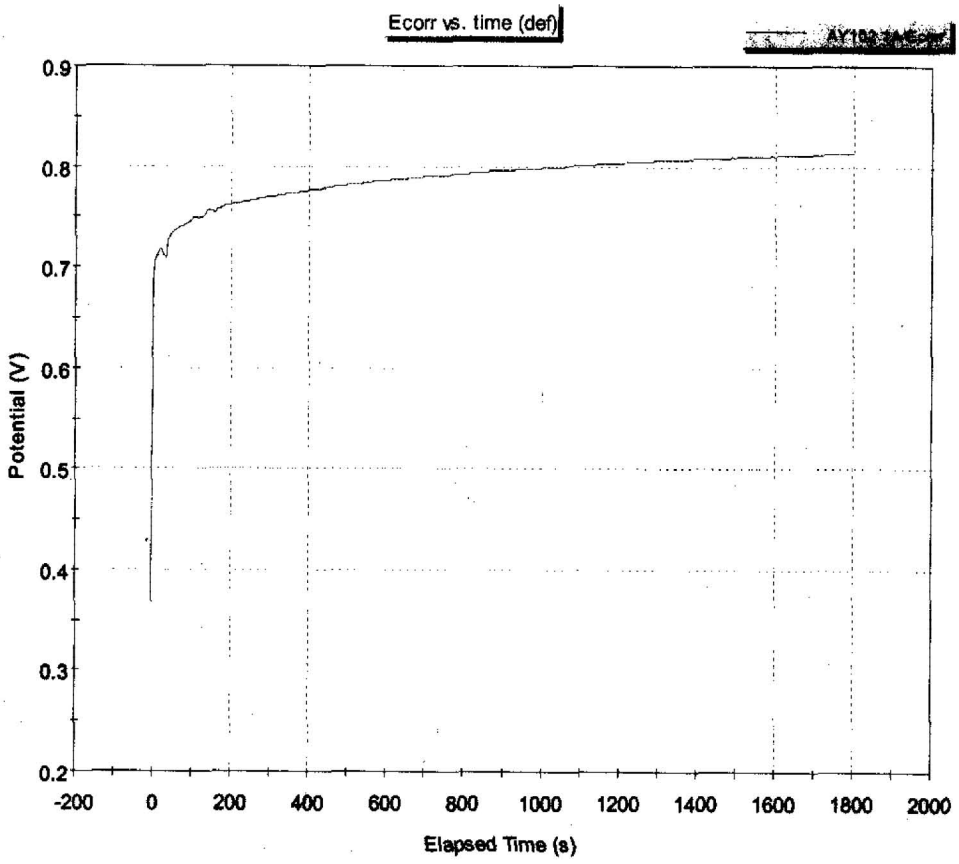

Figure A-4. Coupon S03T001559 Tafel Scan

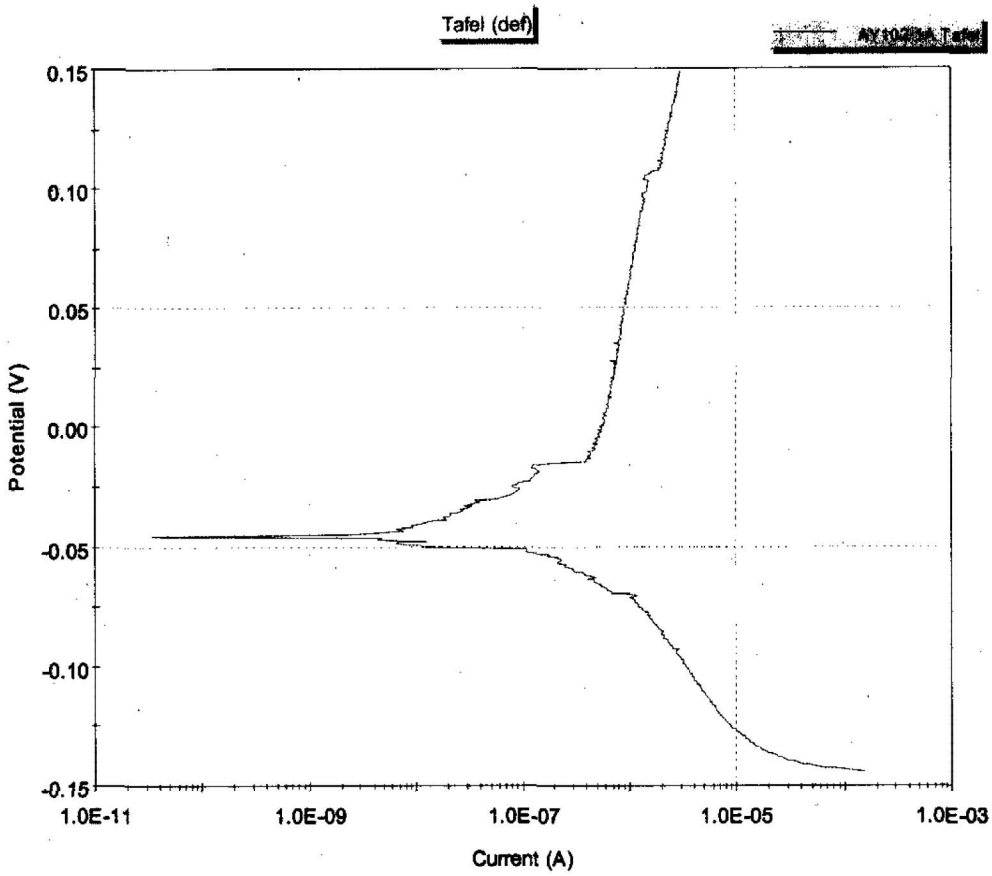

Figure A-5. Coupon S03T001559 Cyclic Polarization Scan

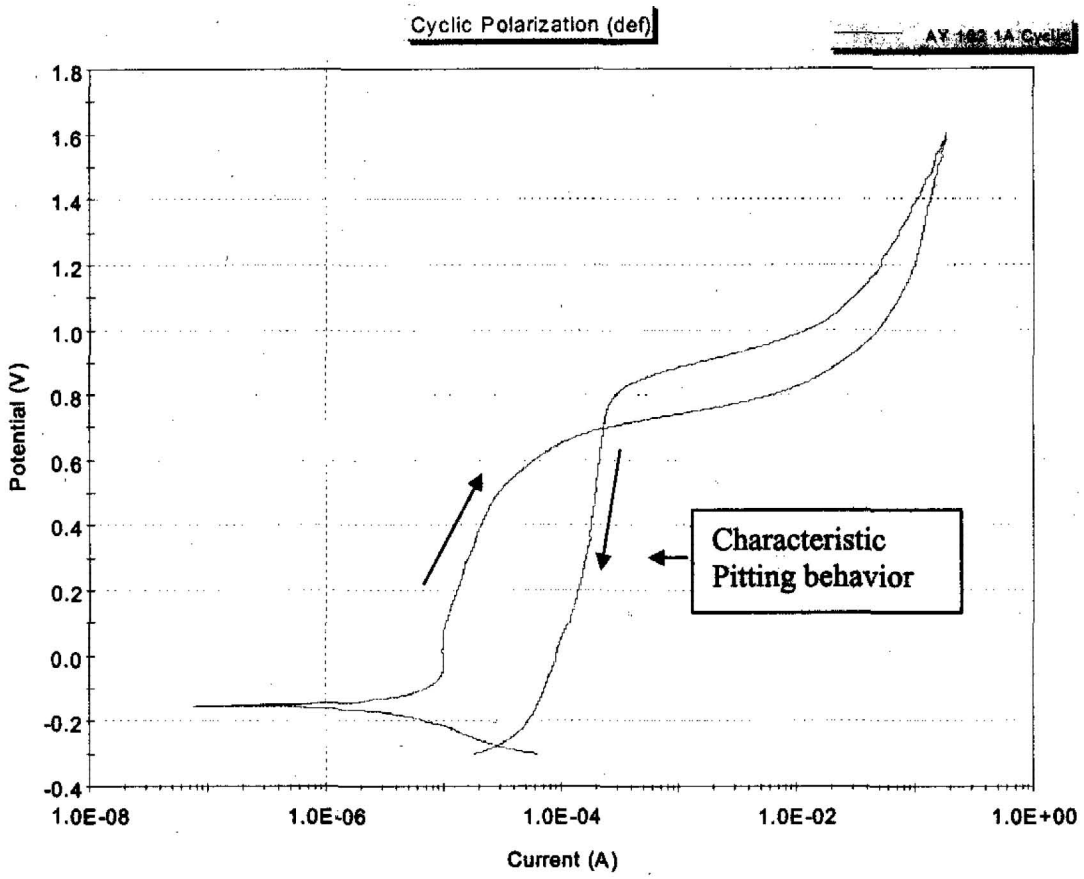

Figure A-6. Coupon S03T001559 Platinum to Platinum Cyclic Scan

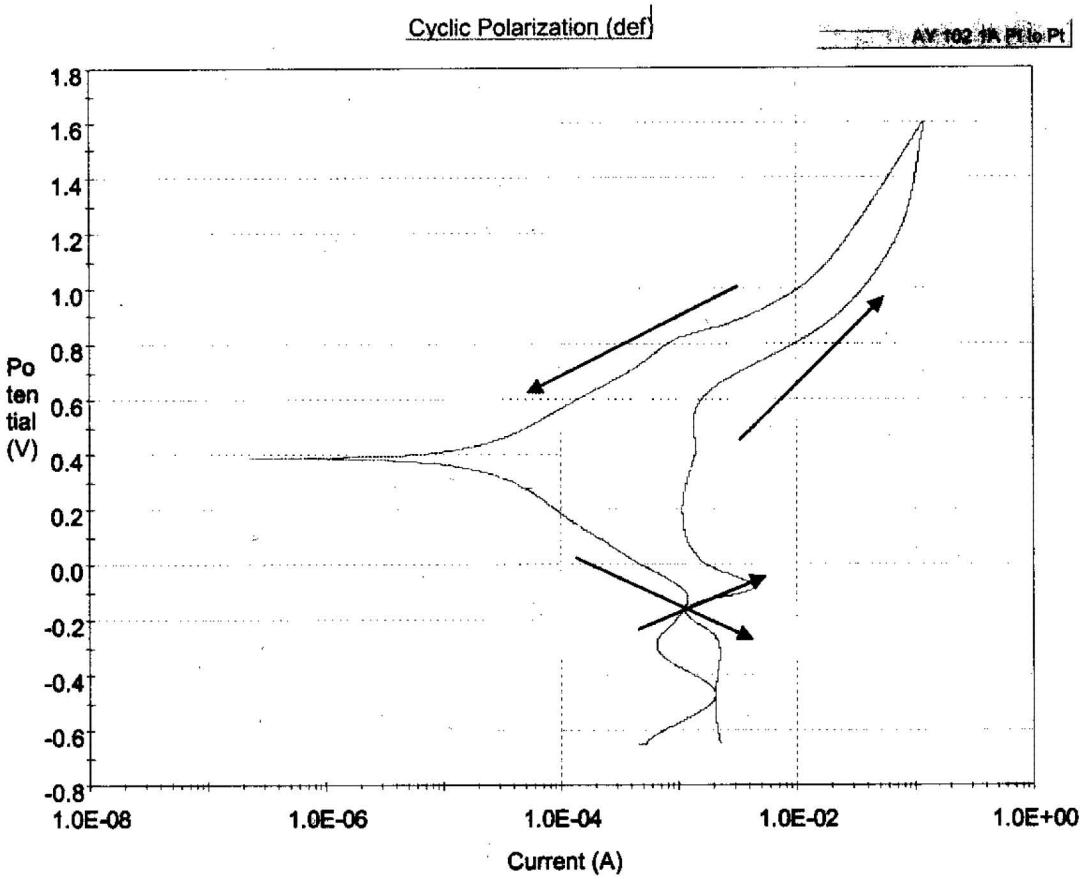

Figure A-7. Coupon S03T001560 E_{corr} versus Time

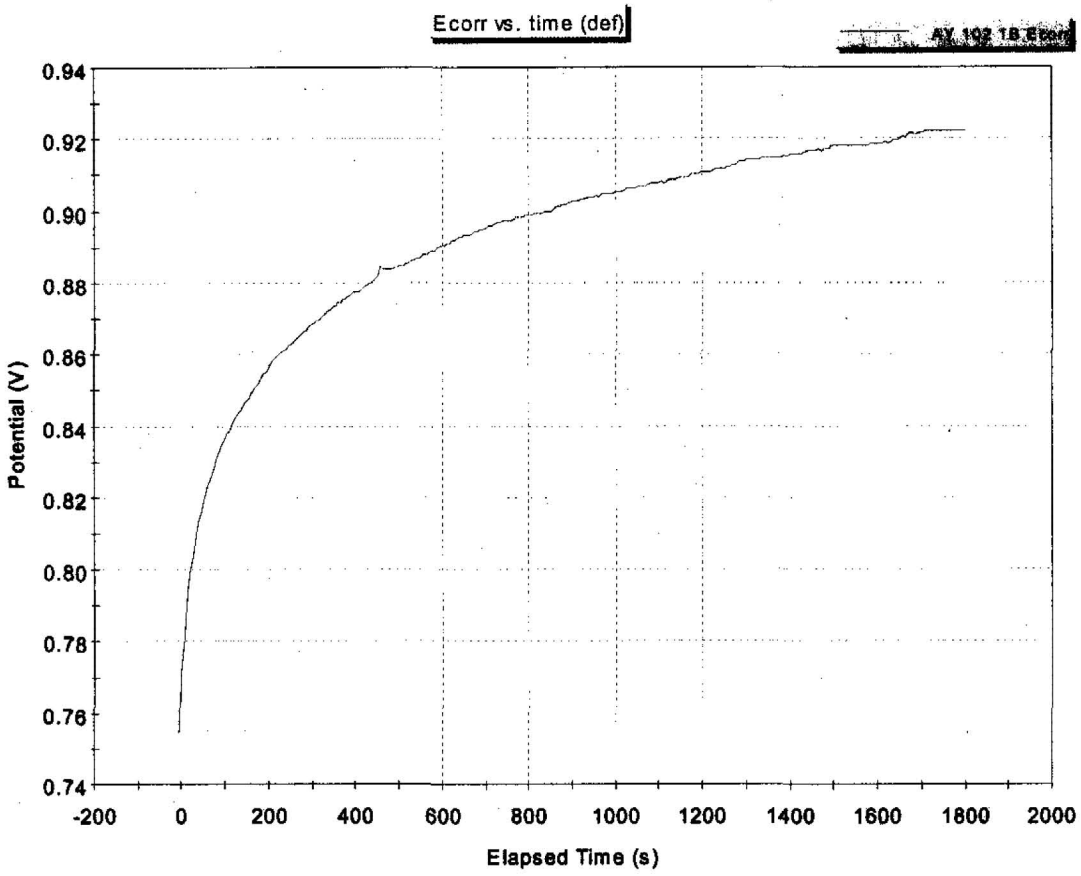

Figure A-8. Coupon S03T001560 Tafel Scan.

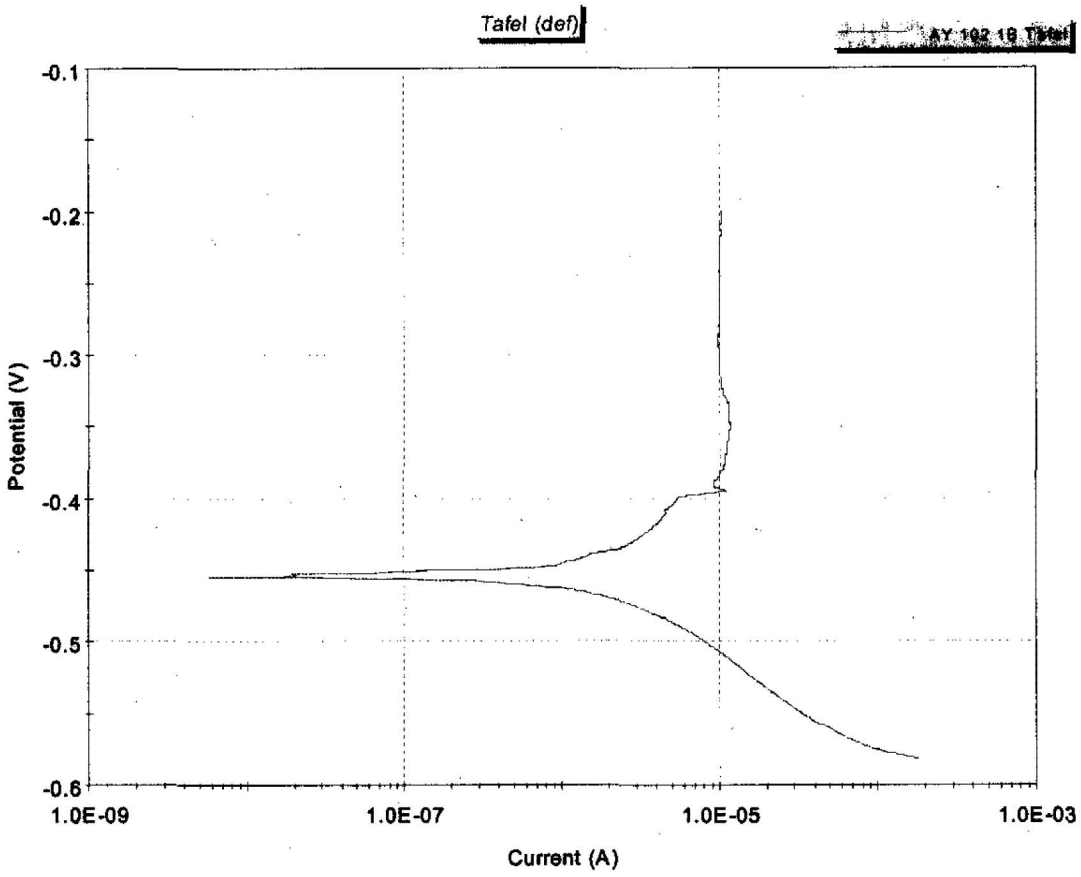

Figure A-9. Coupon S03T001560 Cyclic Polarization Scan

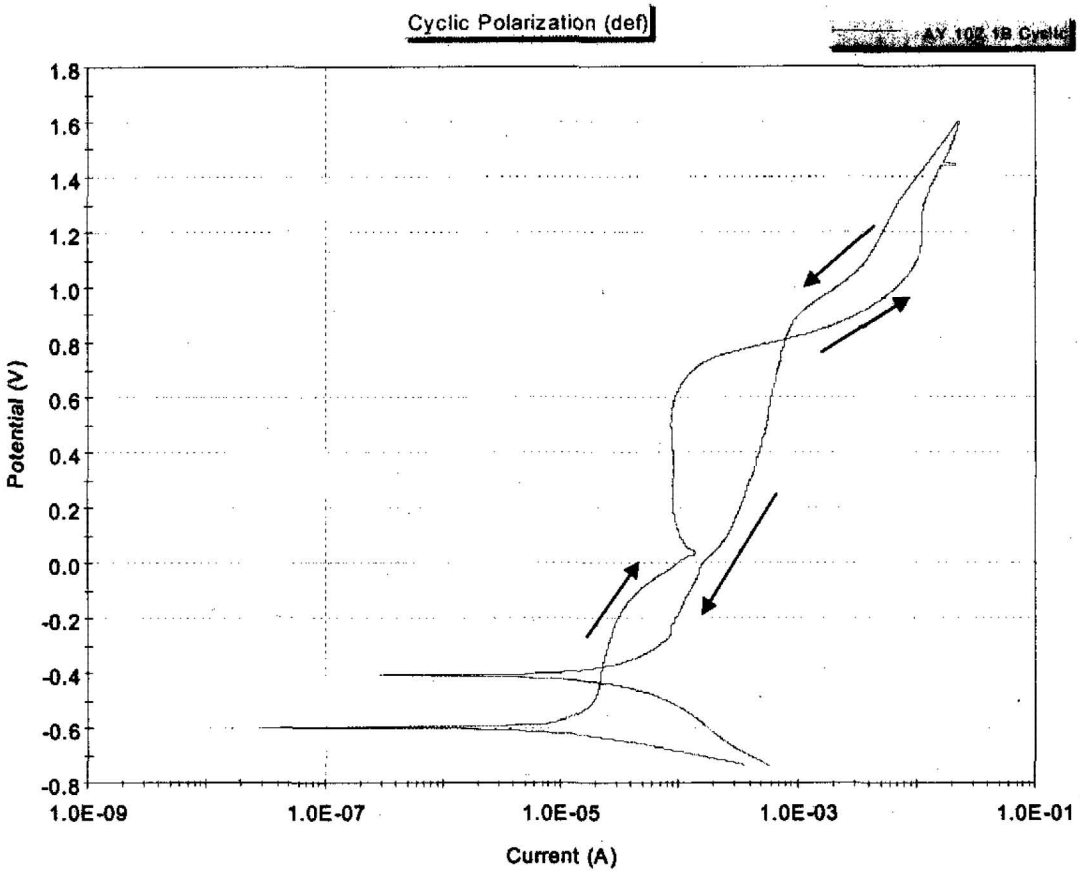

Figure A-10. Coupon S0T001560 Platinum to Platinum Cyclic Scan.

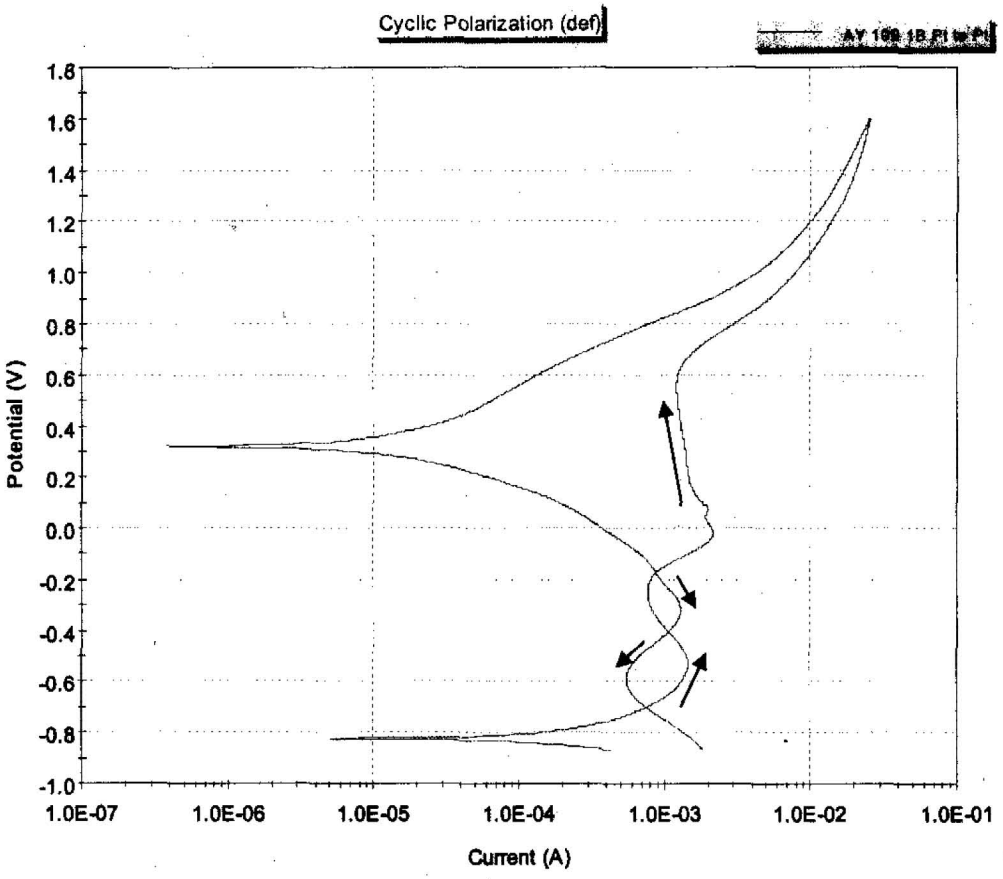

Figure A-11. Coupon 1C Tafel Scan

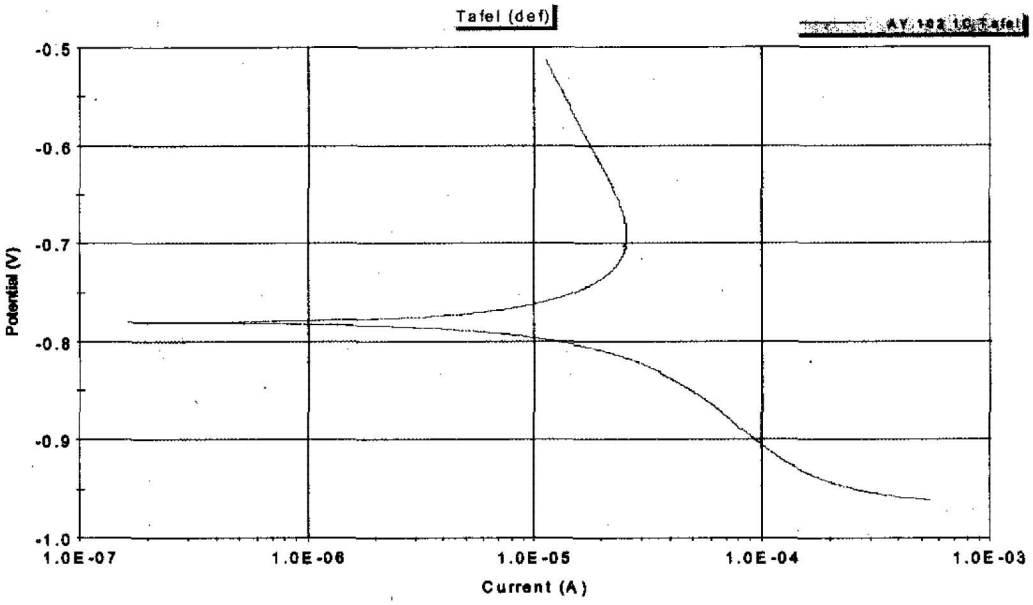

Figure A-12 Coupon 1C Cyclic Polarization Scan

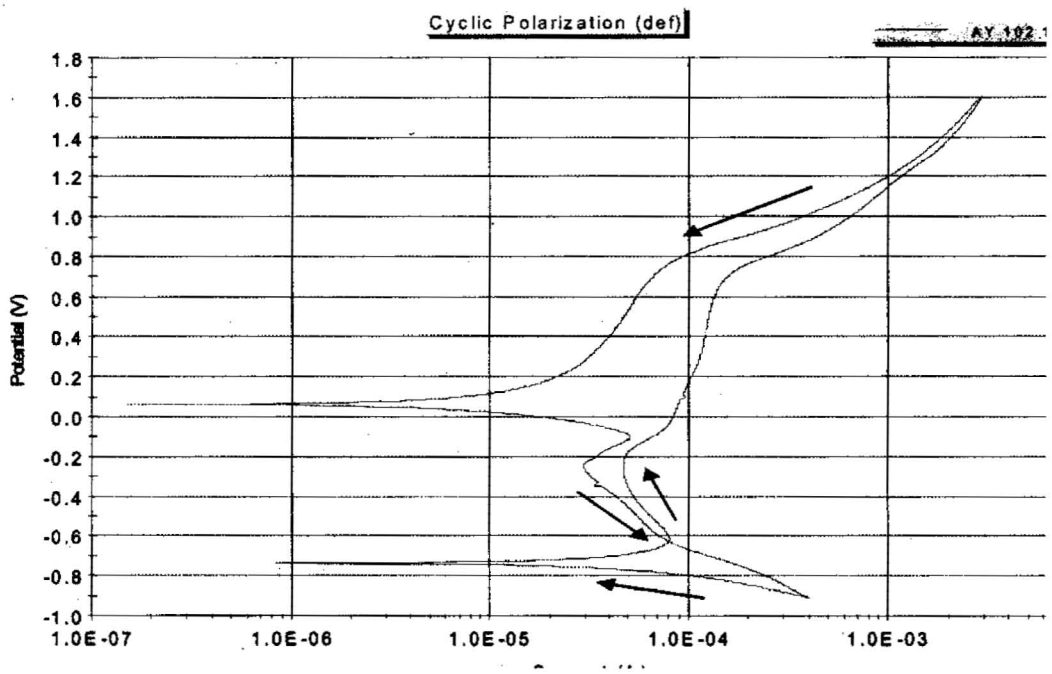

Figure A-13. Coupon 1C Platinum to Platinum Cyclic

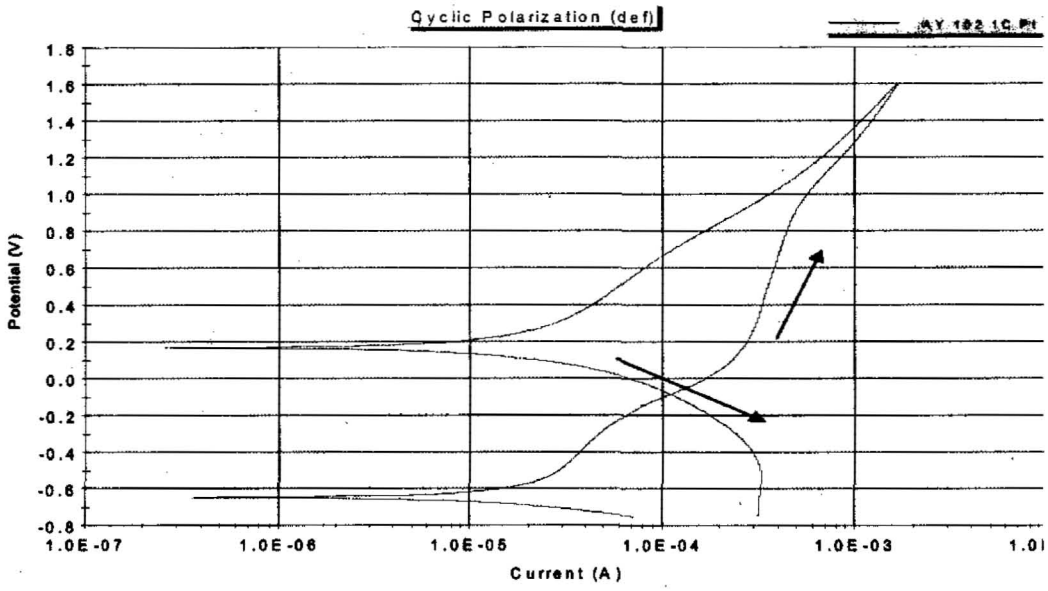

Figure A-14. Coupon 1D Tafel Scan

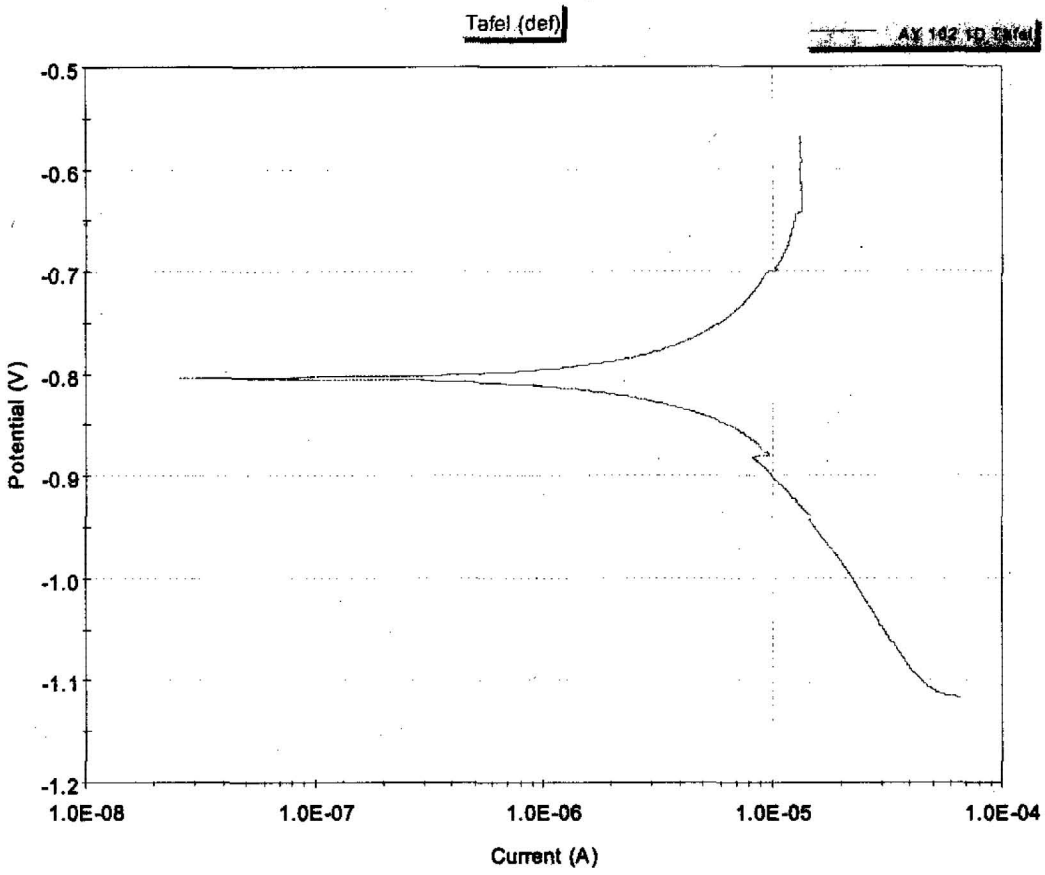

Figure A-15. Coupon 1D Cyclic Polarization

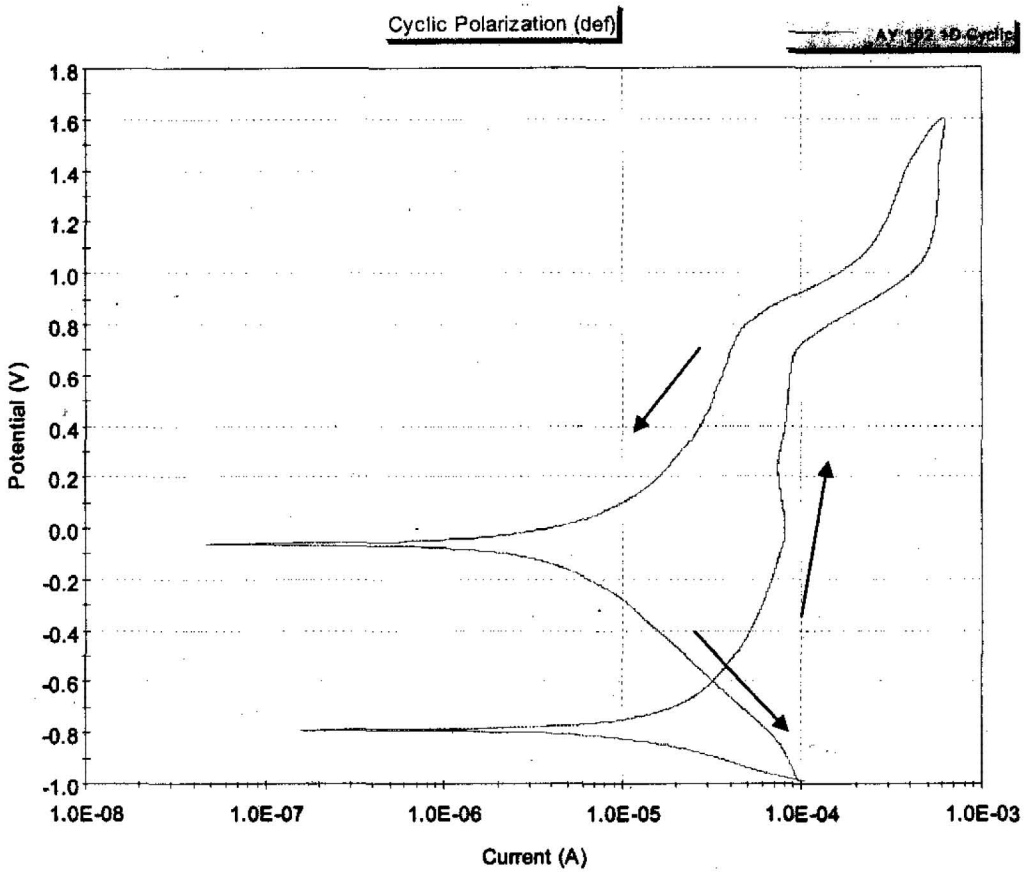

Figure A-16. Coupon 1D Platinum to Platinum Cyclic

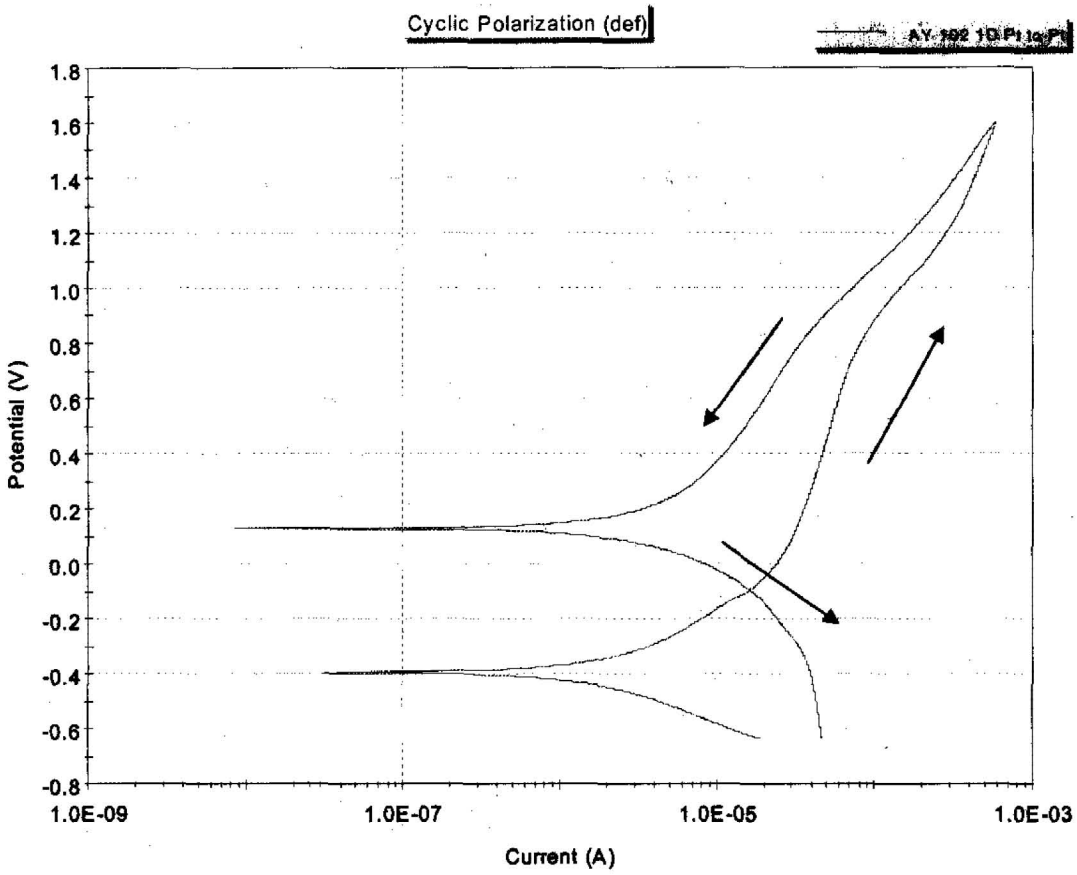

Figure A-17. Coupon S03T001727 Chronoamperometry at 100 mV versus E_{corr} for eighteen hours.

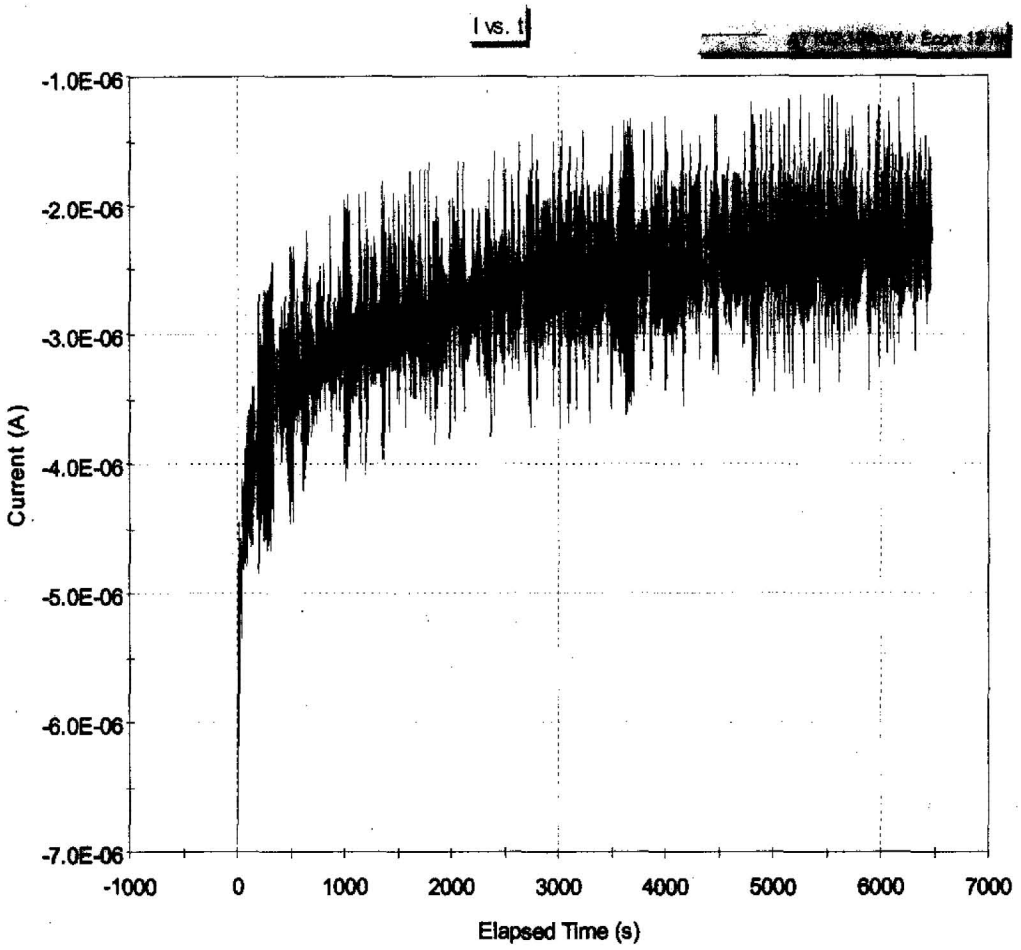

Figure A-18. Coupon S03T001859 E_{corr} versus Time.

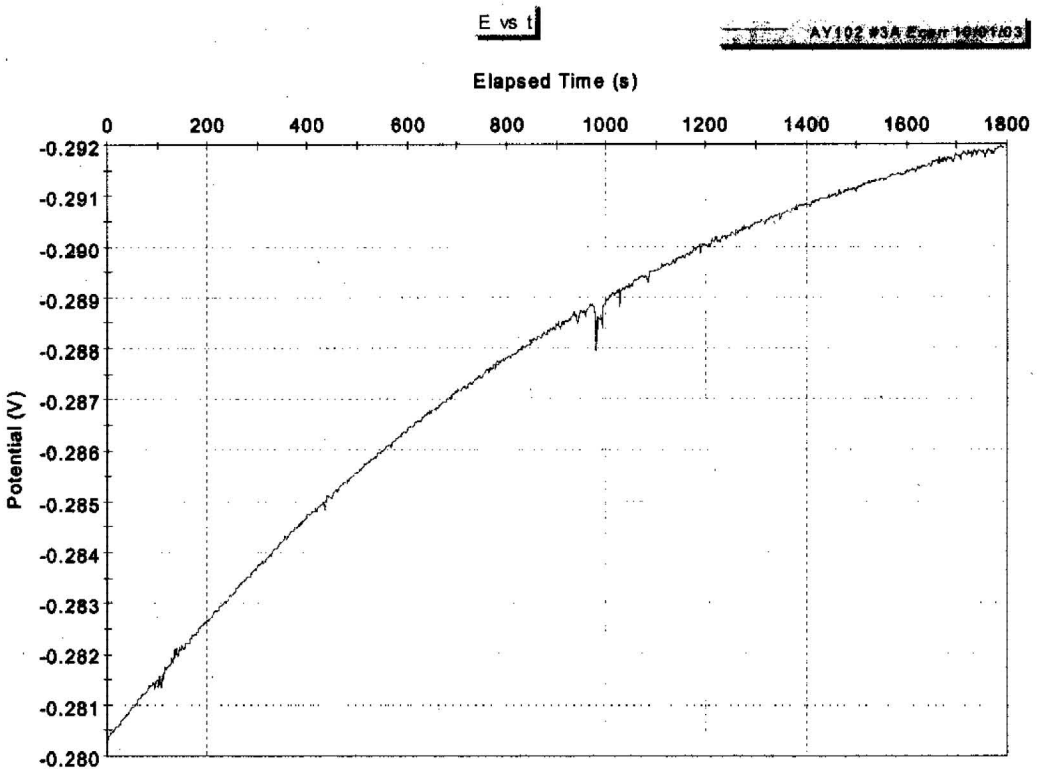

Figure A-19. Coupon S03T001859 Tafel Scan

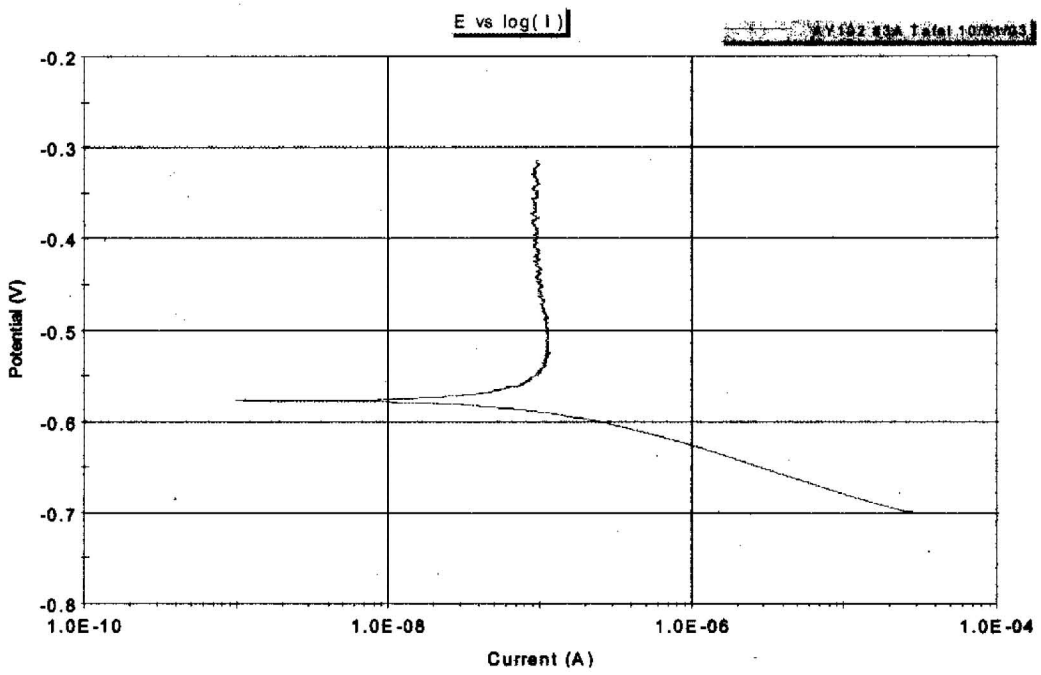

Figure A-20. Coupon S03T001859 Cyclic Polarization.

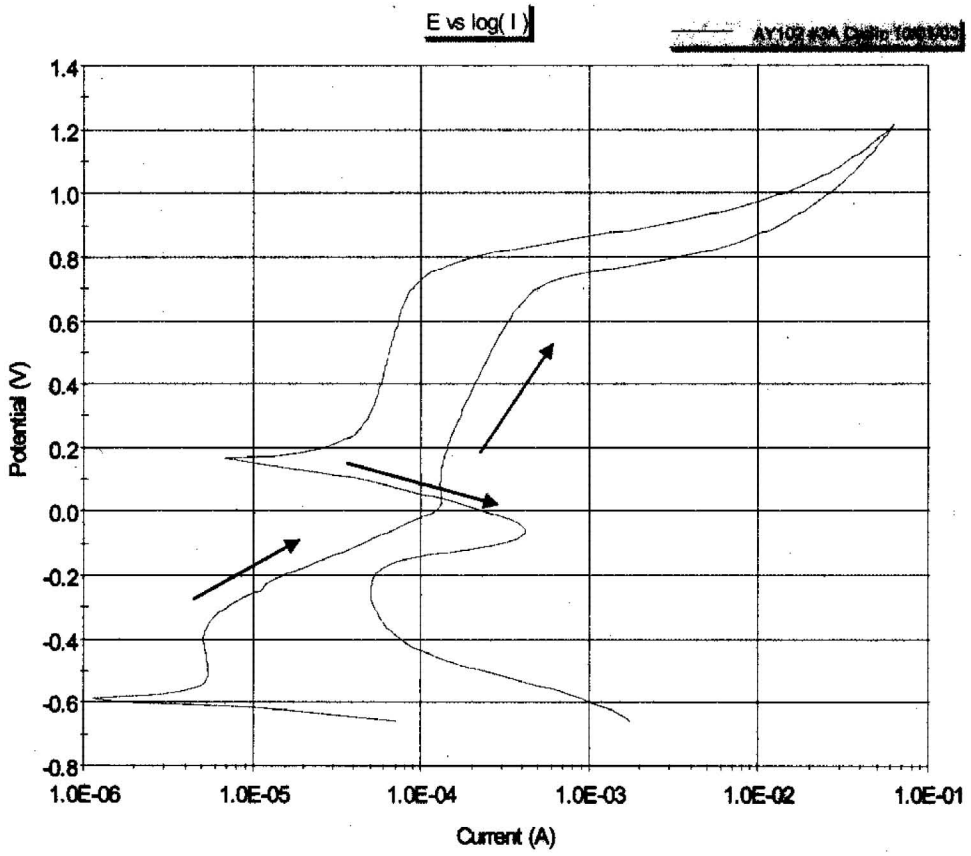

Figure A-21. Coupon S03T001859 Platinum to Platinum Cyclic.

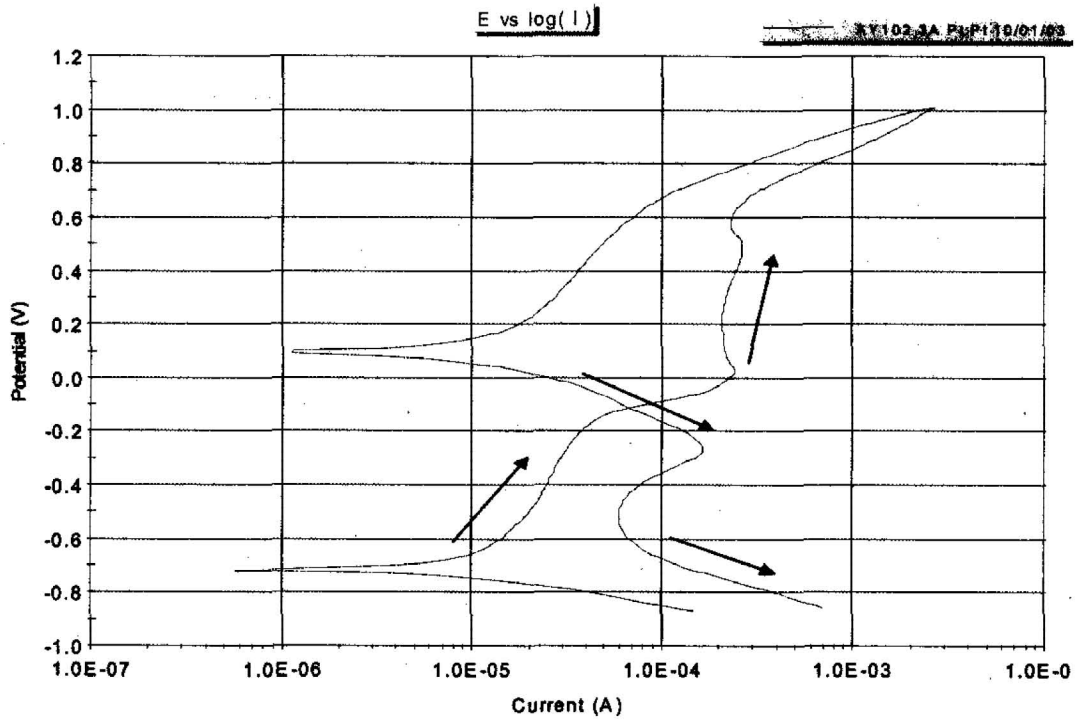

Figure A-22. Coupon S03T001860 E_{corr} versus Time.

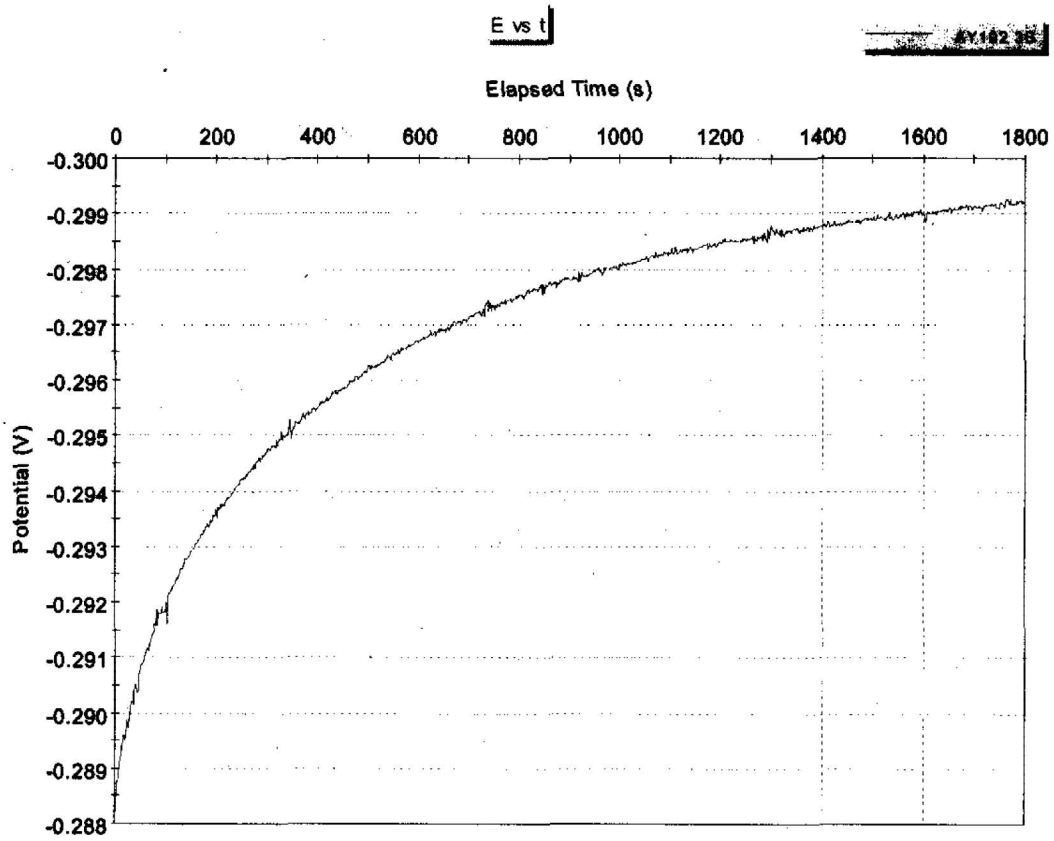

Figure A-23. Coupon S03T001860 Tafel Scan.

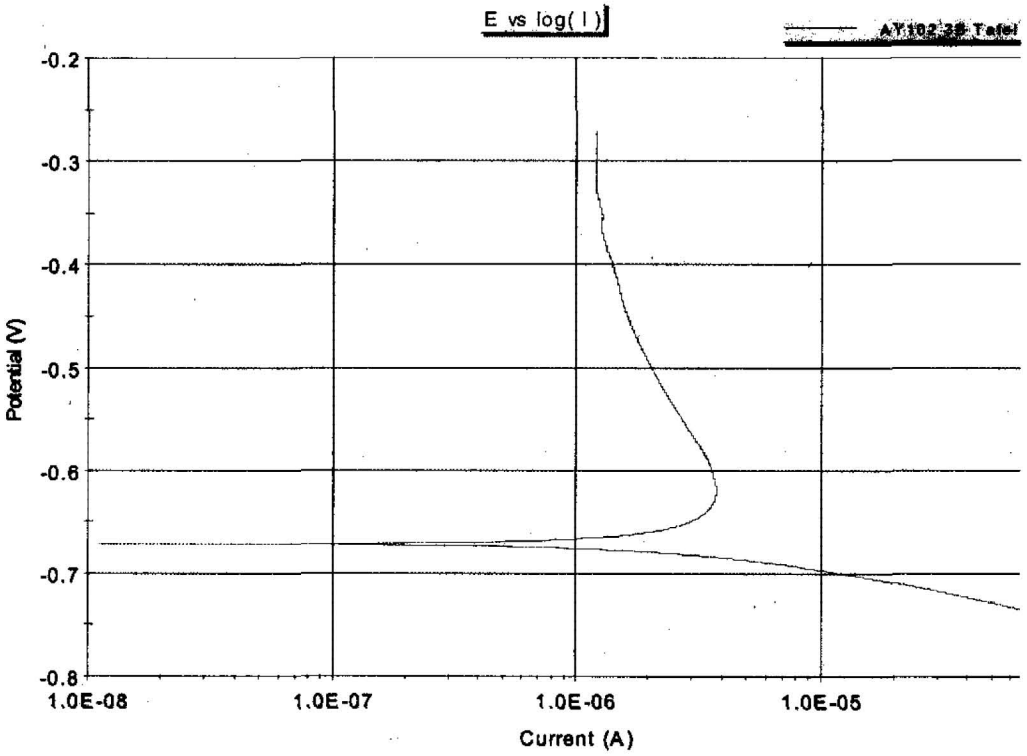

Figure A-24. Coupon S03T001860 Cyclic Polarization.

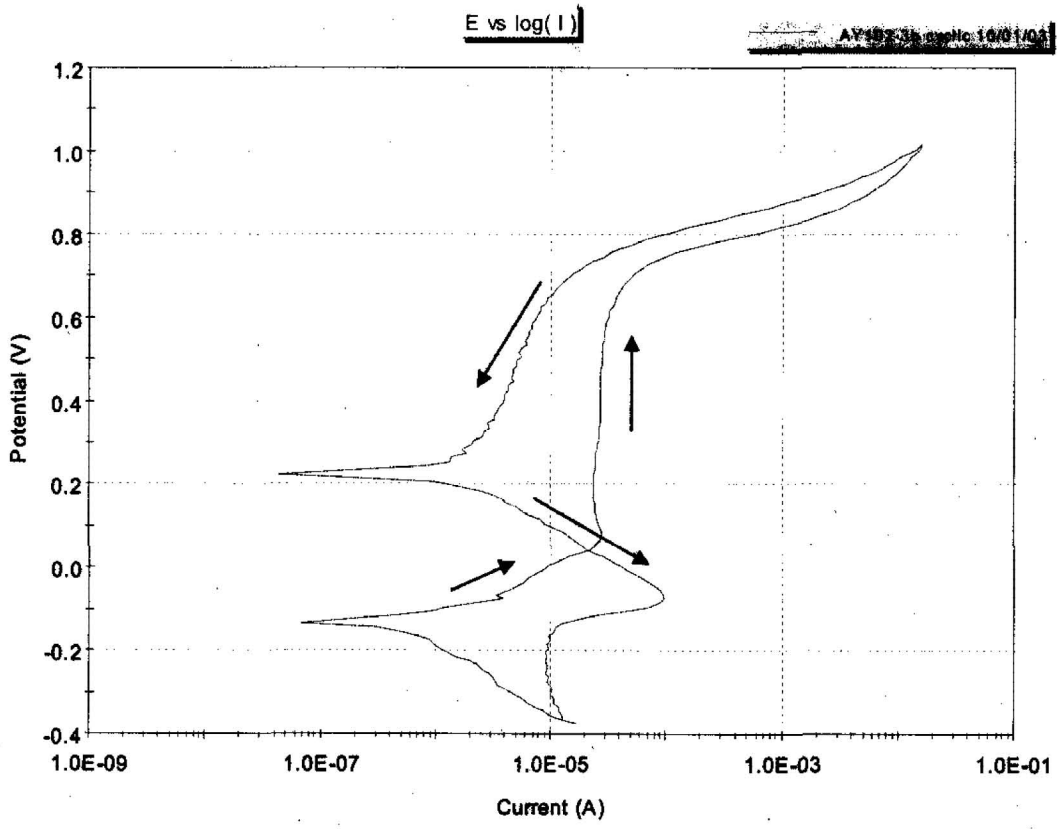

Figure A-25. Coupon S03T001860 Platinum to Platinum Cyclic.

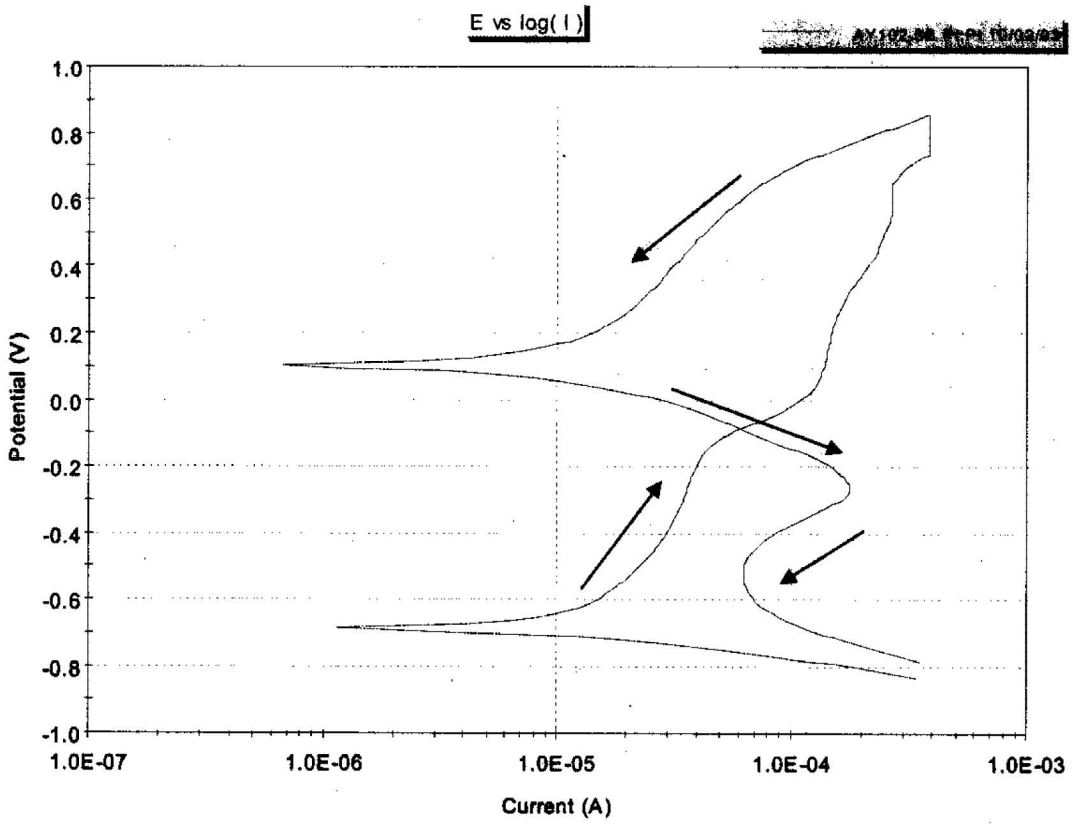

Figure A-26. Coupon S03T001868 E_{corr} versus Time.

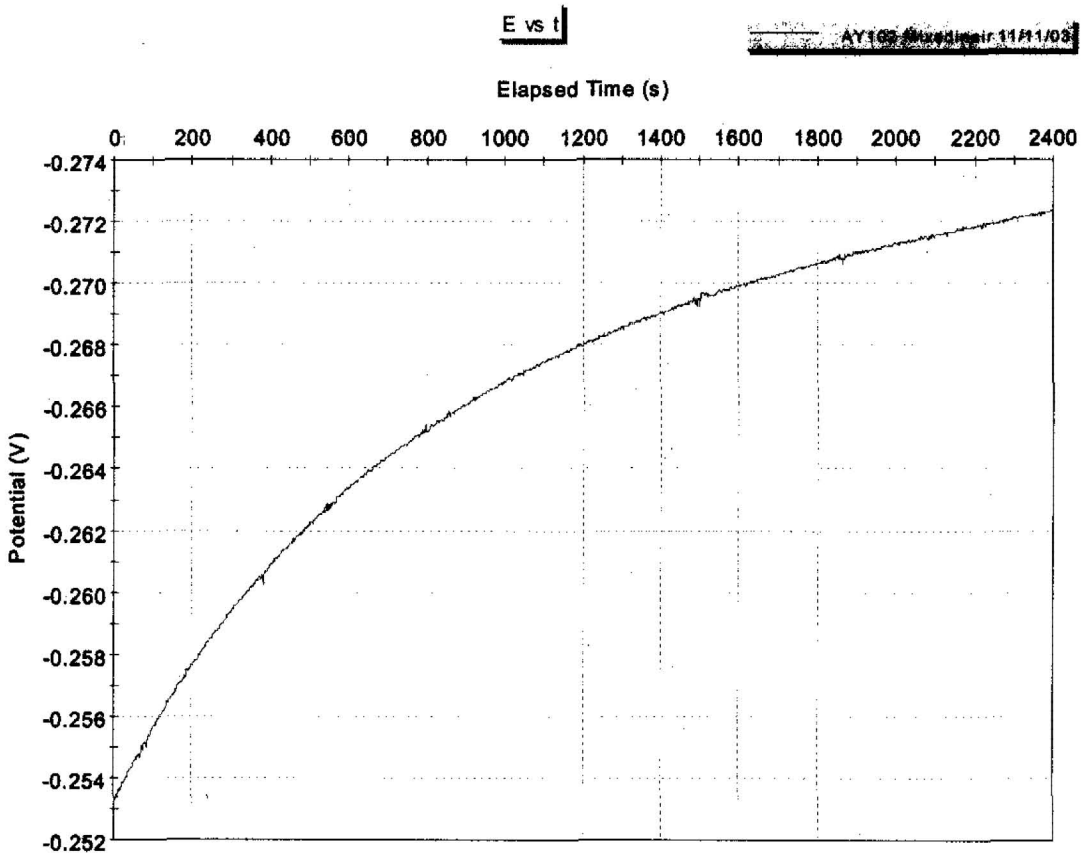

Figure A-28. Coupon S03T001868 Tafel Scan.

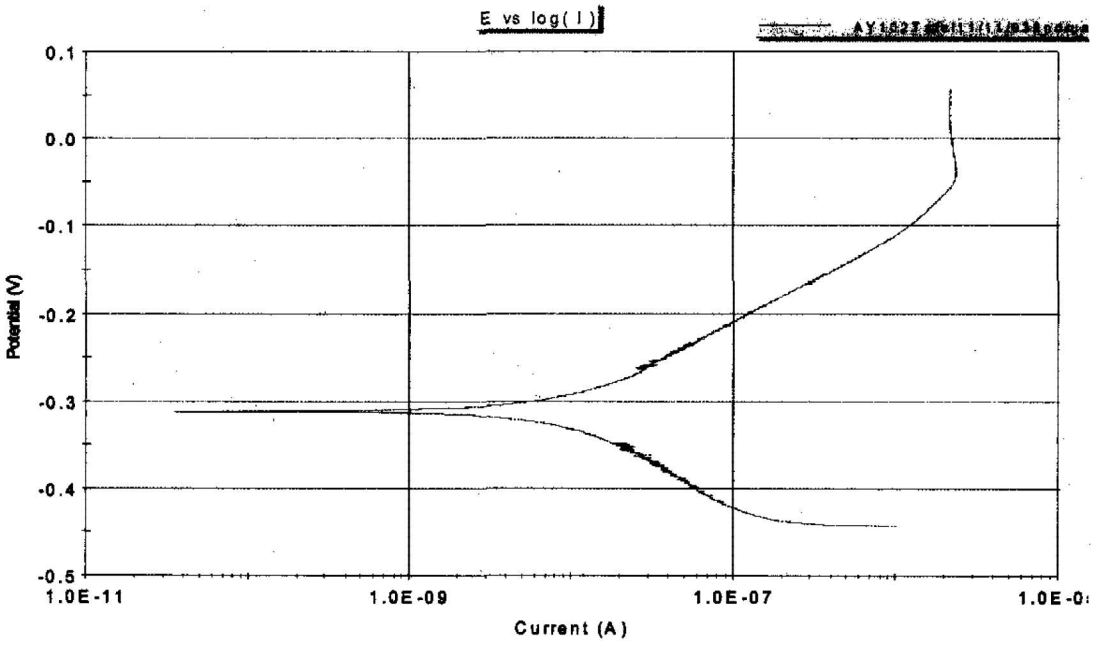

Figure A-29. Coupon S03T001868 Cyclic Polarization.

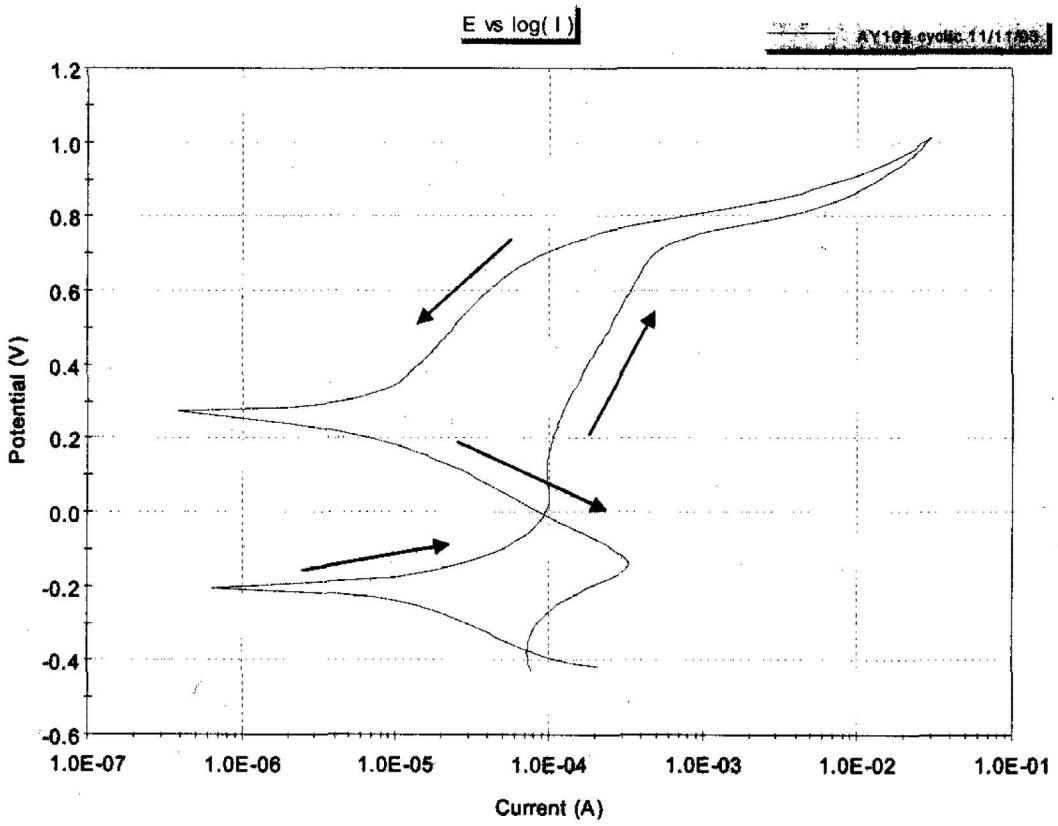

Figure A-30. Coupon S03T001868 Platinum to Platinum Cyclic.

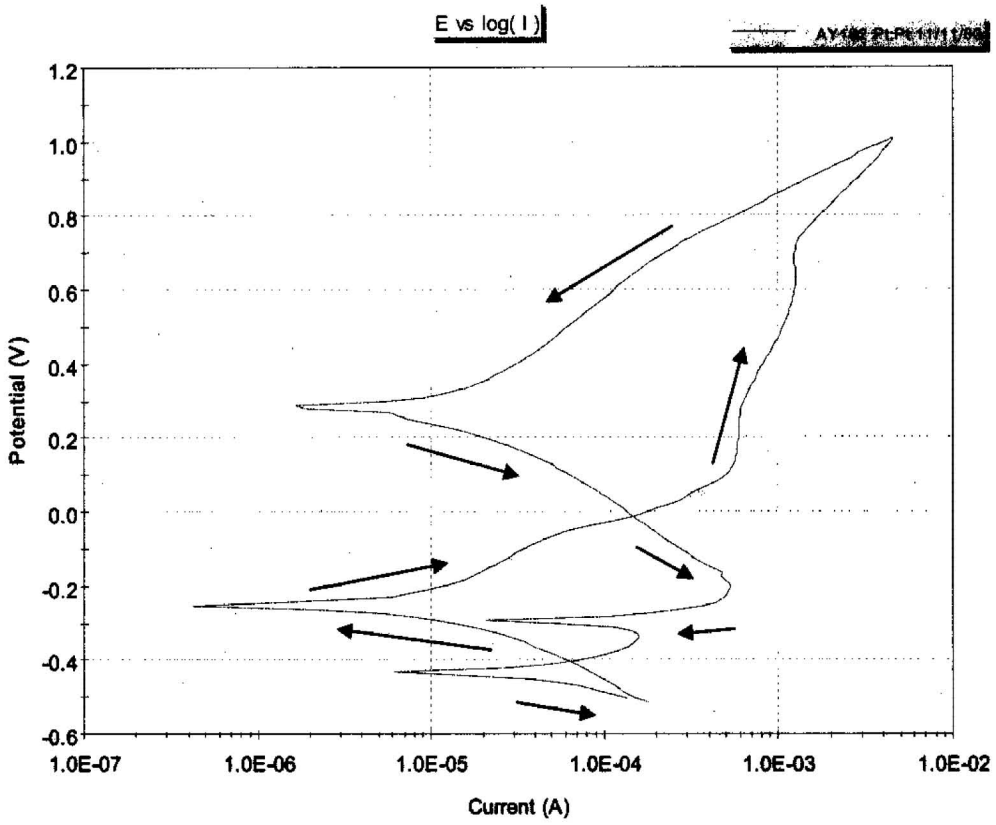

Figure A-31. Coupon S03T001869 E_{corr} versus Time.

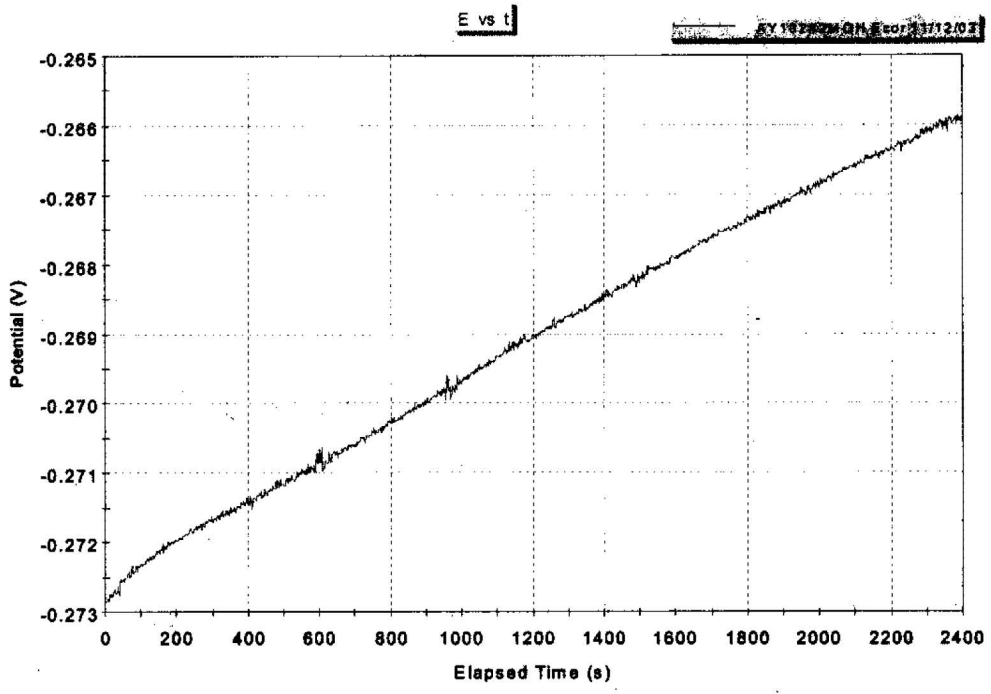

Figure A-32. Coupon S03T001869 Tafel Scan.

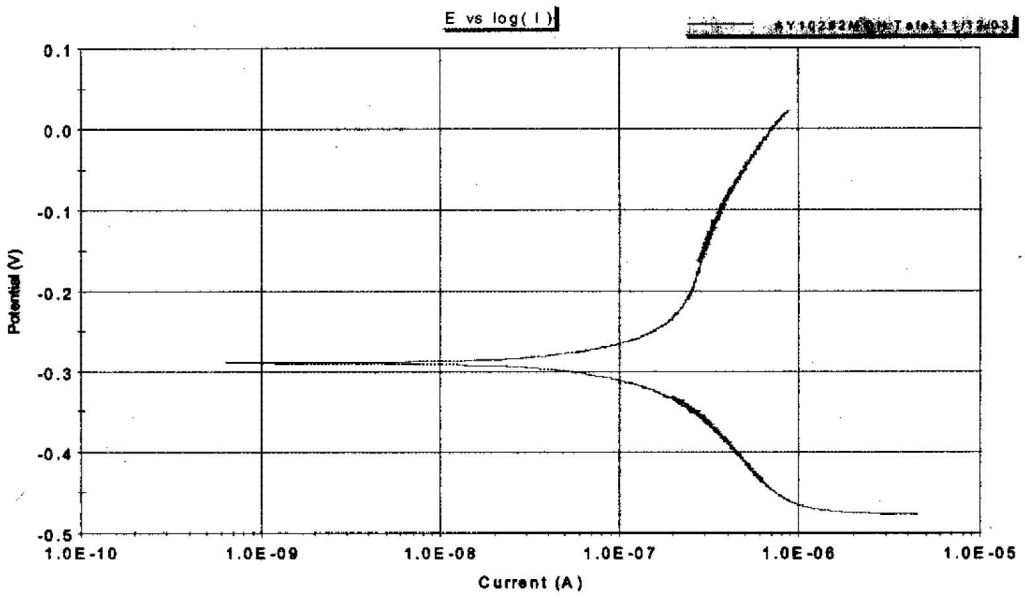

Figure A-33. Coupon S03T001869 Cyclic Polarization Scan.

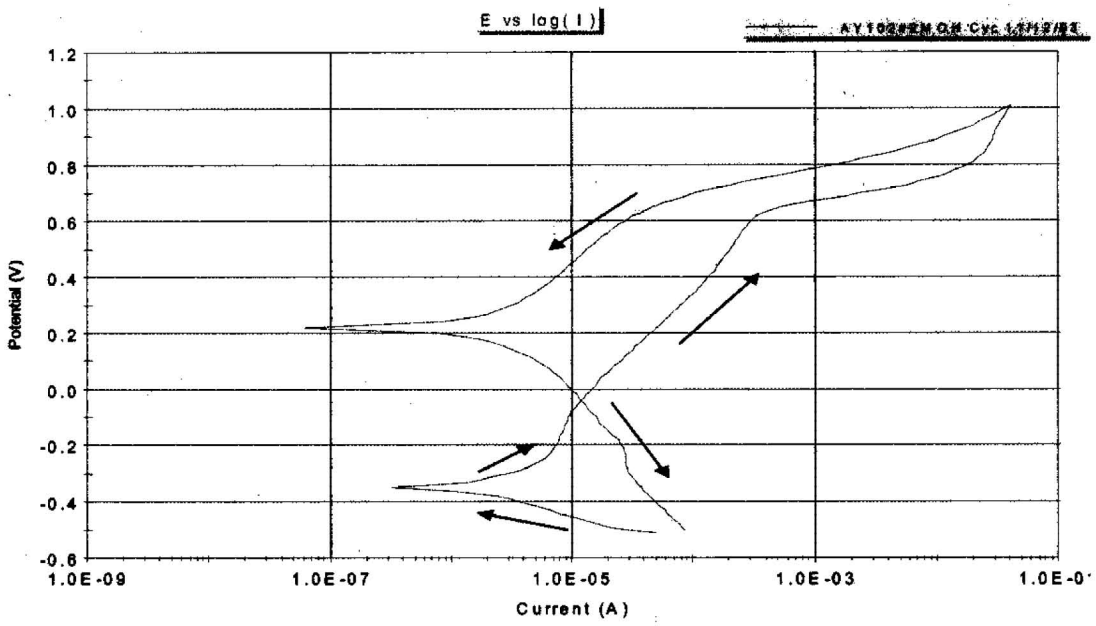

Figure A-34. Coupon S03T001869 Platinum to Platinum Cyclic.

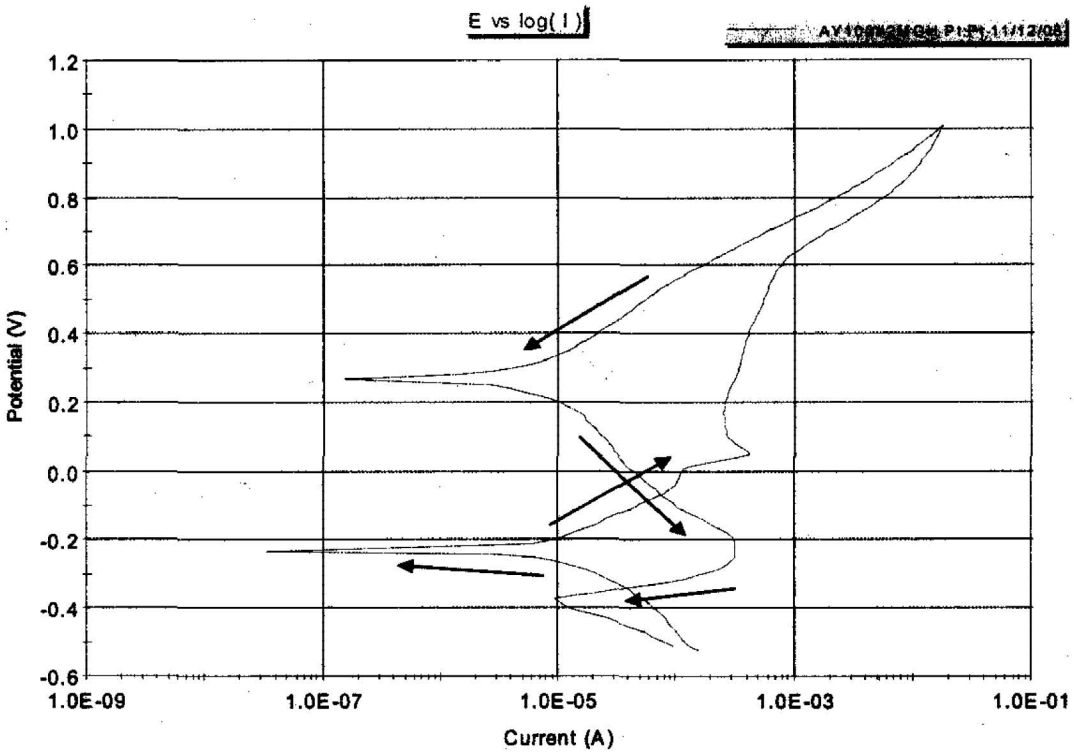

APPENDIX B

SCANNING ELECTRON MICROSCOPY RESULTS

Analytical Process Development used Scanning Electron Microscopy (SEM) to examine several steel corrosion coupons used in testing from the Tank 241-AY-102 anaerobic electrochemical corrosion project. The extent and nature of corrosion and the products of corrosion were documented.

The samples are identified as follows:

Sample I.D.	Description	Received in Lab	Analysis Dates
S03T001559	C308 S14R2 1A	08/22/2003	08/26 & 9/11/2003
S03T001560	C308 S14R2 1B	08/22/2003	10/17/2003
S03T001561	C308 S14R2 1C	08/22/2003	not analyzed
S03T001562	C308 S14R2 1D	08/22/2003	not analyzed
S03T001727	C308 S14R1 2A	09/10/2003	09/11/2003
S03T001859	C308 S14R1 3A	10/02/2003	10/17/2003
S03T001860	C308 S14R1 3B	10/02/2003	10/20/2003
S03T001868	C308 S14R1 1M	10/16/2003	10/17/2003
S03T001869	C308 S14R1 2MOH	10/16/2003	10/20/2003
Control 515		09/10/2003	09/11/2003

The cylindrical coupons were rinsed in the 11A Hotcells, placed in a jar of inhibited water and transferred to room 2B in the 222-S Laboratory. In the laboratory, each coupon was sonicated with distilled water. Each coupon was dried and any remaining removable contamination was removed by wiping with clean tissues. A twisted piece of tissue was used to dry the threaded hole at the top of each coupon. The coupons were then stored in small brown manila folders until analysis.

For SEM analysis, the coupons were mounted with an adhesive carbon disk onto the SEM stage. The coupons were mounted with the axis of the cylinder parallel to the surface of the stage. Prior to mounting, each coupon was visually inspected for the greatest incidence of potential corrosion (rough, sometimes yellowish-orange regions) along the outer surface parallel to the axis. The portion of the surface that had the most possible corrosion spots was mounted so that this was the surface examined on the SEM.

Analysis was conducted at 20 kV on an ASPEX Personal SEM equipped with a light element Energy Dispersive Spectrometer (EDS) capable of detecting carbon any heavier elements.

Images were acquired in Secondary Electron Imaging (SEI) and Backscattered Electron Imaging (BEI) modes. Secondary electrons are sensitive to topography and surface texture, while backscattered electrons are sensitive to chemistry, with regions having heavier atomic weight elements appearing brighter.

The images in this Appendix are organized from the least affected by corrosion to the most affected. They begin with an untested control sample, below.

The surface of the control sample coupon was not exposed to the tank waste or subjected to electrochemical cycling. It was prepared for SEM analysis by removing from it's wrapper and mounting directly on the SEM.

The original parallel scratches of the polished surface show clearly in both the SEI (Figure B-1, left) and BEI (Figure B-1 right) imaging mode. Some of the grooves appear to be compressed or folded (Figure B-2), perhaps by polishing the surface after the grooves had formed.

Figure B-1. SEI (left) and BEI (right) SEM images of Control 515.

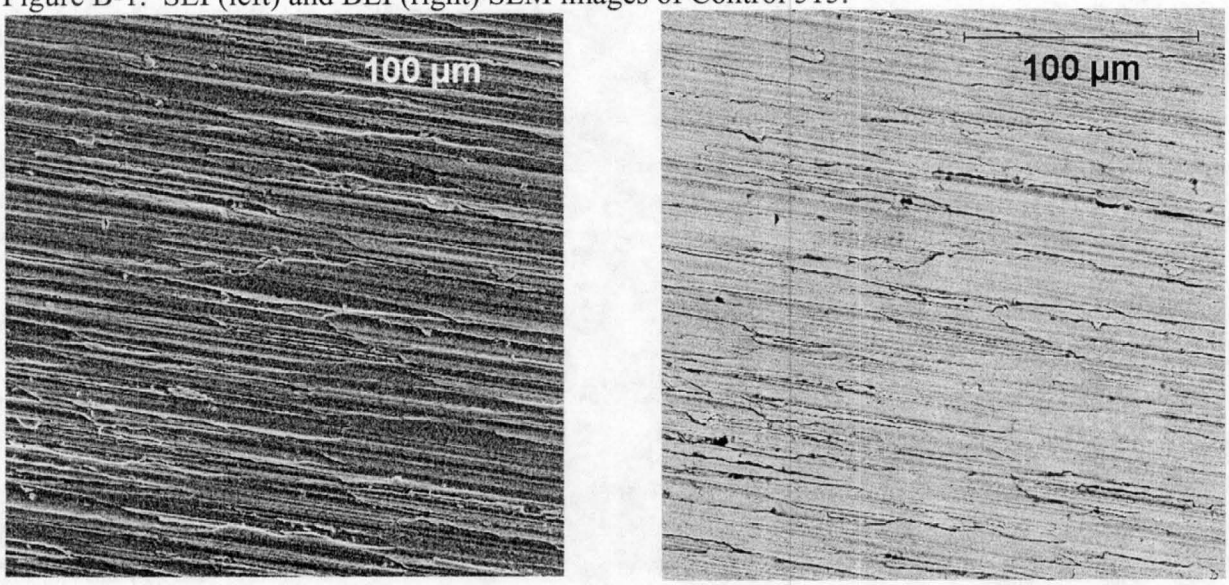

Figure B-2. Higher magnification BEI (right) SEM image of Control 515.

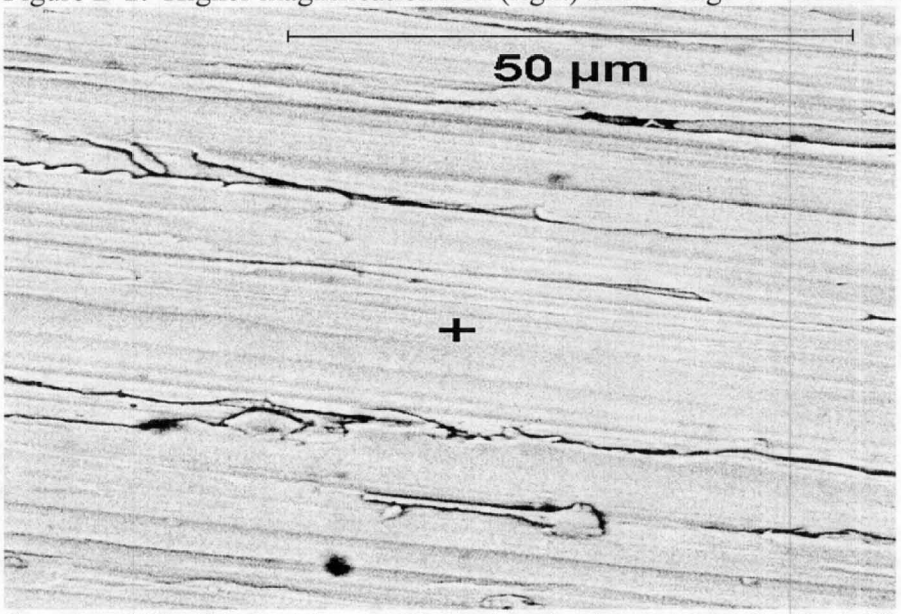

Samples S03T001868 (Coupon 1M, mixed in air) and S03T001869 (Coupon 2MOH, mixed with tank 241-AY-102 supernatant), also showed little or no evidence for corrosion. No obvious patches of corrosion were observed visually, so the portion of the surface that was examined in the SEM was random. SEM examination of the entire length of these two coupons revealed no obvious corrosion (Figures B-3 and B-4)

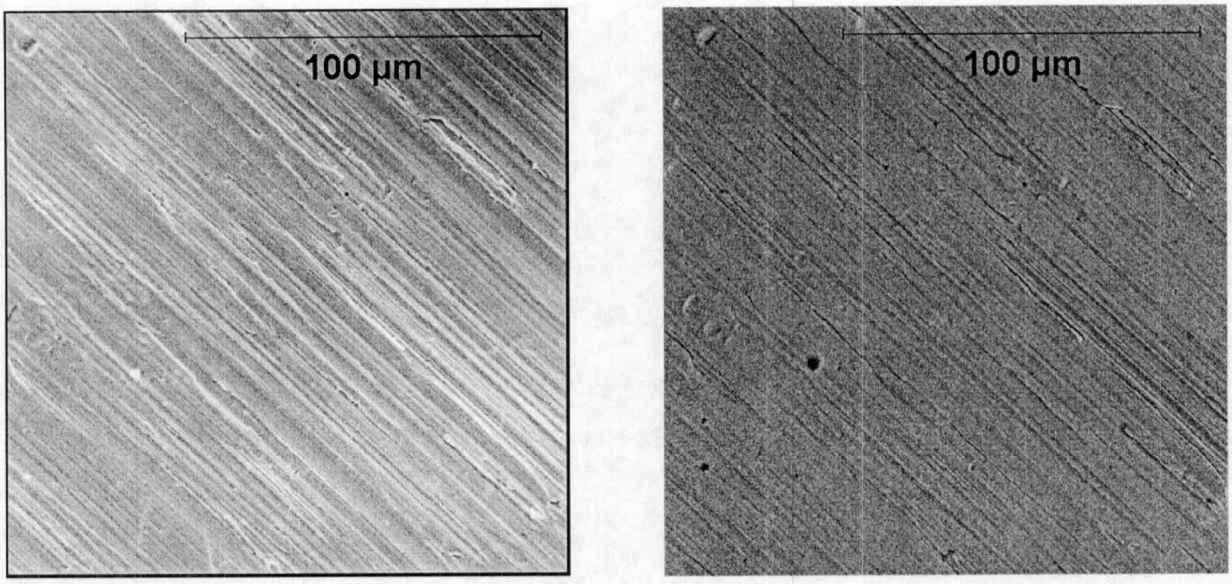

Figure B-3. SEI (left) and BEI (right) SEM images of Sample S03T001868 (Coupon 1M).

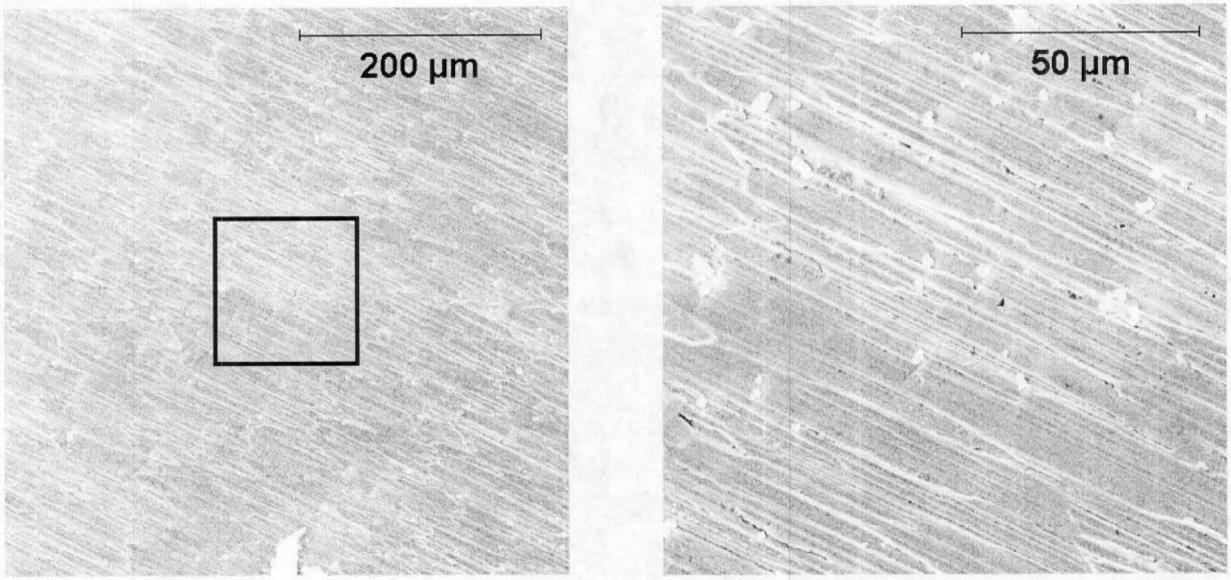

Figure B-4. Low Magnification SEI (left) SEM image of Sample S03T001869 (Coupon 2MOH). Area outlined in box is expanded in the SEI image to the right.

Sample coupon S03T001860 (Coupon 3B, room temperature scan) showed one small patch of yellow-orange corrosion during the visual examination. This was on the surface that was mounted for SEM examination. The SEM revealed no other patches along the length of the coupon and the patch that had been observed visually was difficult to discern using the SEM (Figure B-5). In this figure, a thin, irregular streak extending from the top to the bottom of the images. The normal surface striations seem to continue, for the most part, through the corrosion feature.

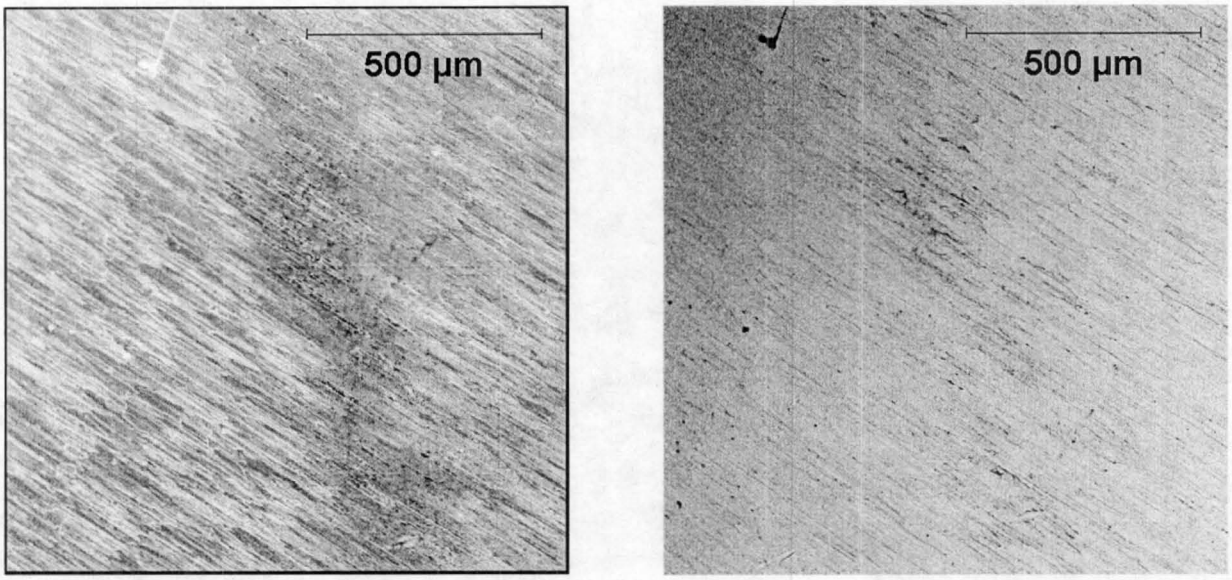

Figure B-5. SEI (left) and BEI (right) SEM images of Sample S03T001860 (Coupon 3B).

Higher magnification images from this patch show that this corroded region is characterized by a deepening of the low spots between the striations (Figure B-6). The gaps between the striations in the corroded region (right-hand portion of each image in Figure B-6) are also darker on the SEI images. This is probably due to an increase in surface roughness in these regions.

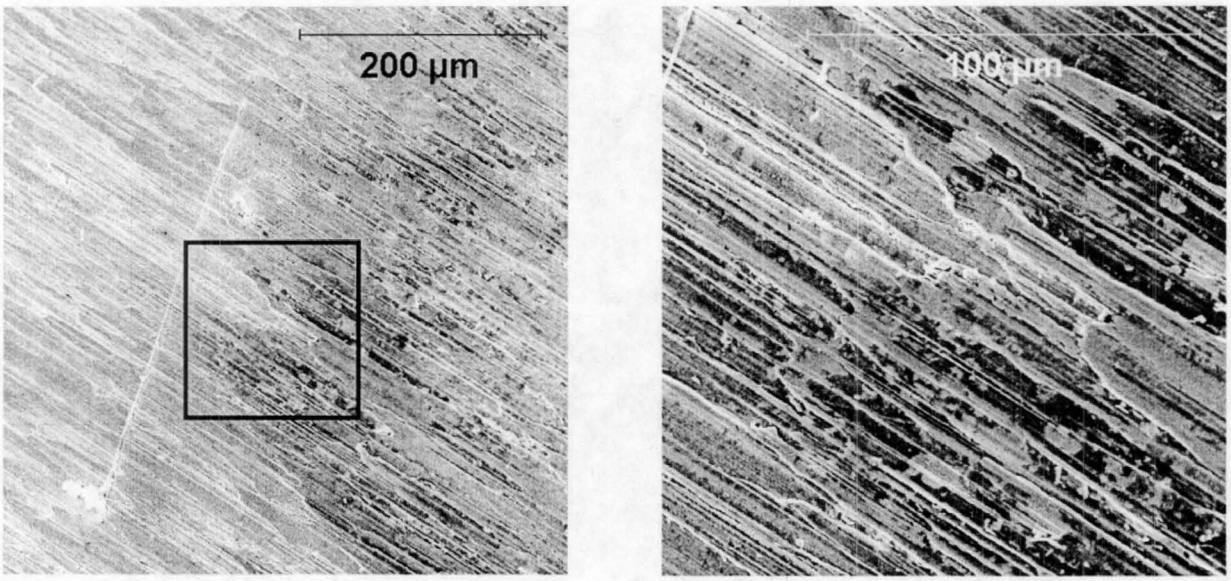

Figure B-6. Low Magnification SEI (left) SEM image of Sample S03T001860 (Coupon 3B). Area outlined in box is expanded in the SEI image to the right.

Sample S03T001727 (Coupon 2A, chronoamperometry) showed a had single large patch in the surface examined on the SEM. The pitting in this patch was obvious, in part because they were partially filled with corrosion products (iron oxides and hydroxides) and they partially obliterated the surface striations.

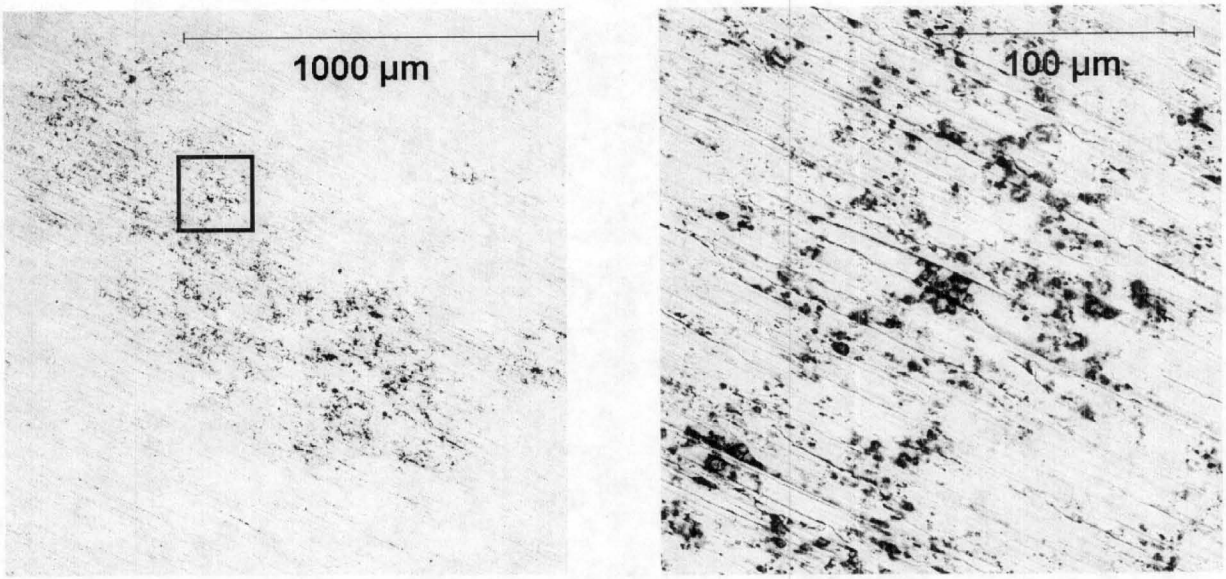

Figure B-7. Low Magnification BEI (left) SEM image of Sample S03T001727 (Coupon 2A). Area outlined in box is expanded in the BEI image to the right.

Sample coupon S03T001859 (Coupon 3A room temperature scan) was characterized by very small corroded regions that were barely visible as dark, rough patches. The side that was mounted up in the SEM had four of these patches. Two of these are shown in Figures B-8 and B-9. The first (Figure B-8) shows a larger area of "staining" with the striations continuing through the darker area in the SEI (left) image similar to Coupon 3B. However, it also shows a smaller region characterized by deep pits. The BEI (right) image in Figure B-7 shows that these pits are partially filled with corrosion product (iron oxides/hydroxides).

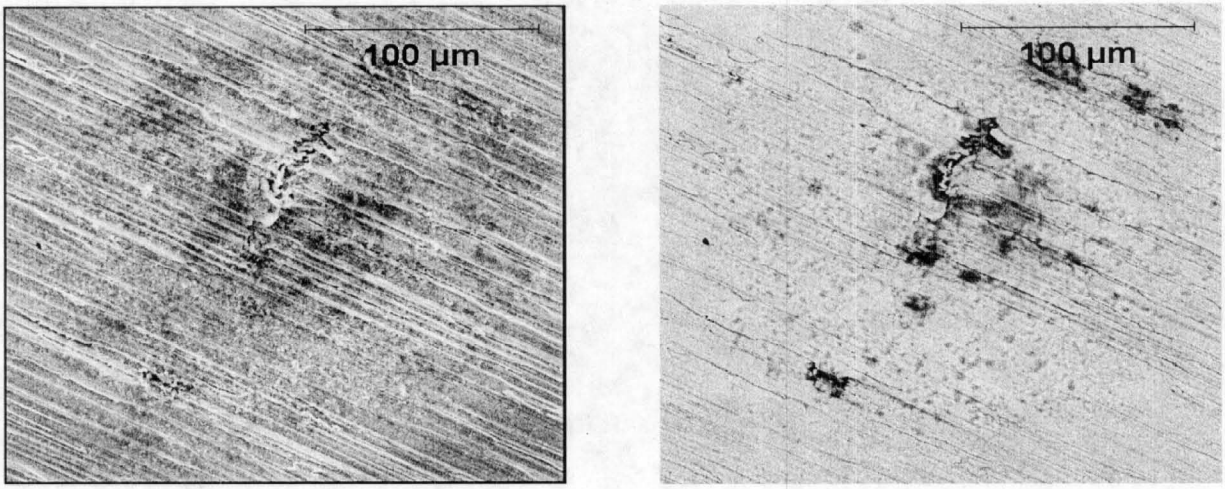

Figure B-8. SEI (left) and BEI (right) SEM images of Sample S03T001859 (Coupon 3A).

The other three pitted areas are similar to the one illustrated in Figure B-9, a small patch of deep, coalescing pits.

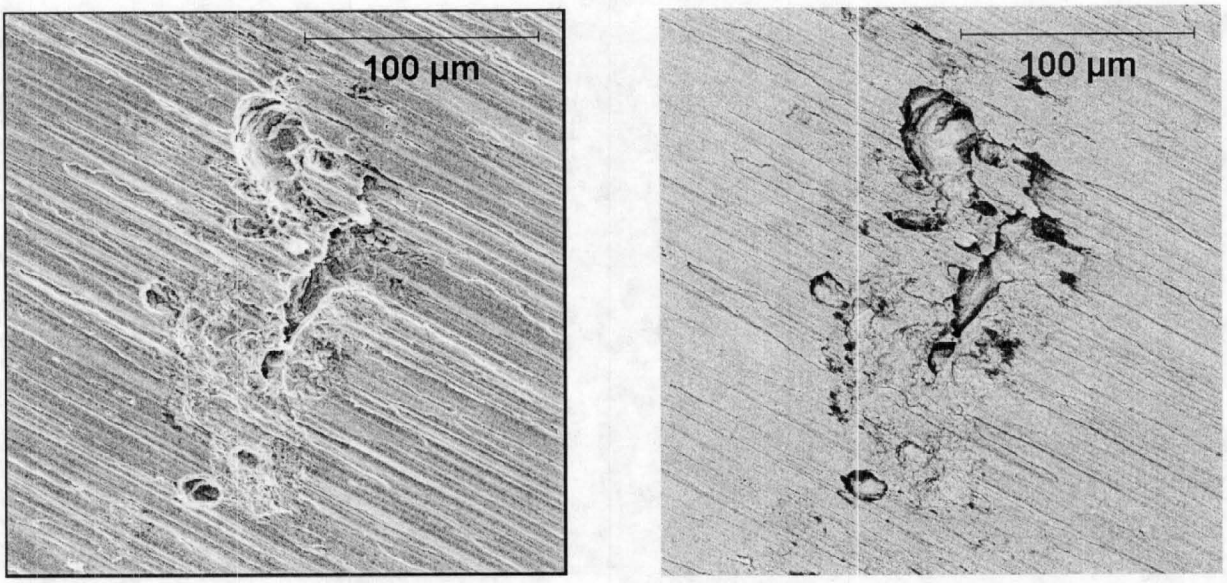

Figure B-9. SEI (left) and BEI (right) SEM images of Sample S03T001859 (Coupon 3A).

Sample S03T001560 (Coupon 1B high temperature scan, segment 14R2) and Sample S03T001559 (Coupon 1A high temperature scan, segment 14R2) both showed several very large patches that were severely affected by corrosion. These patches were one or more millimeters across (greater than 1000 microns).

Figure B-10 shows the edge of one of these patches on sample S03T001560 (Coupon 1B). Here the surface striations are still visible, bit they are etched below the depth of the original sample surface.

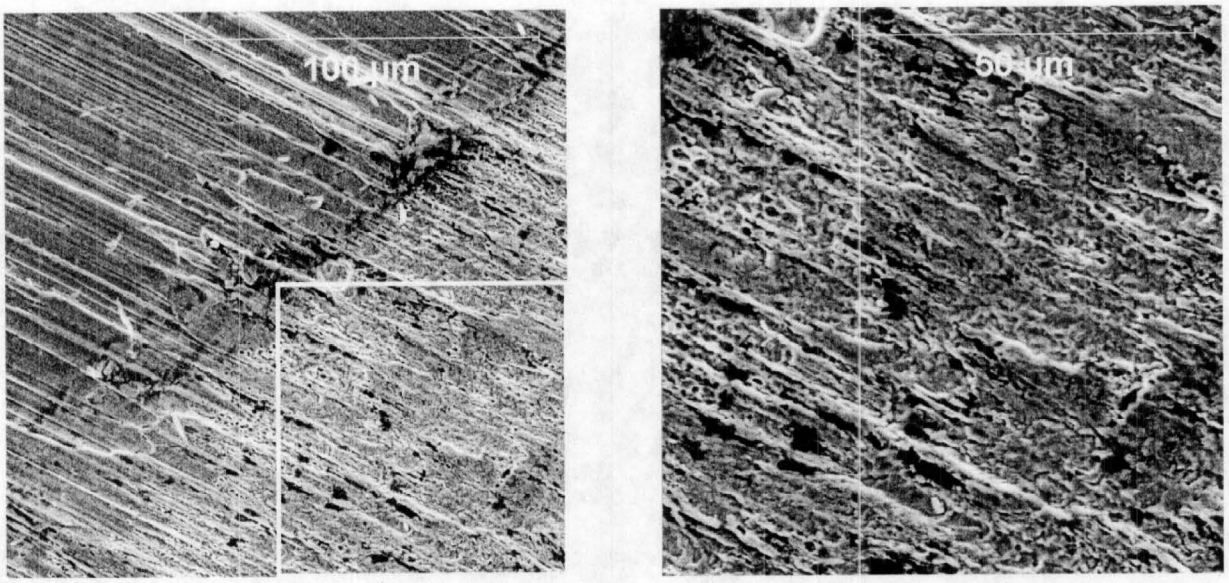

Figure B-10. Medium Magnification SEI (left) SEM image of Sample S03T001560 (Coupon 1B). Area outlined in box is expanded in the SEI image to the right.

In another portion of the same large patch, the etching and pitting has completely eaten away any evidence of the original surface features (Figure B-11).

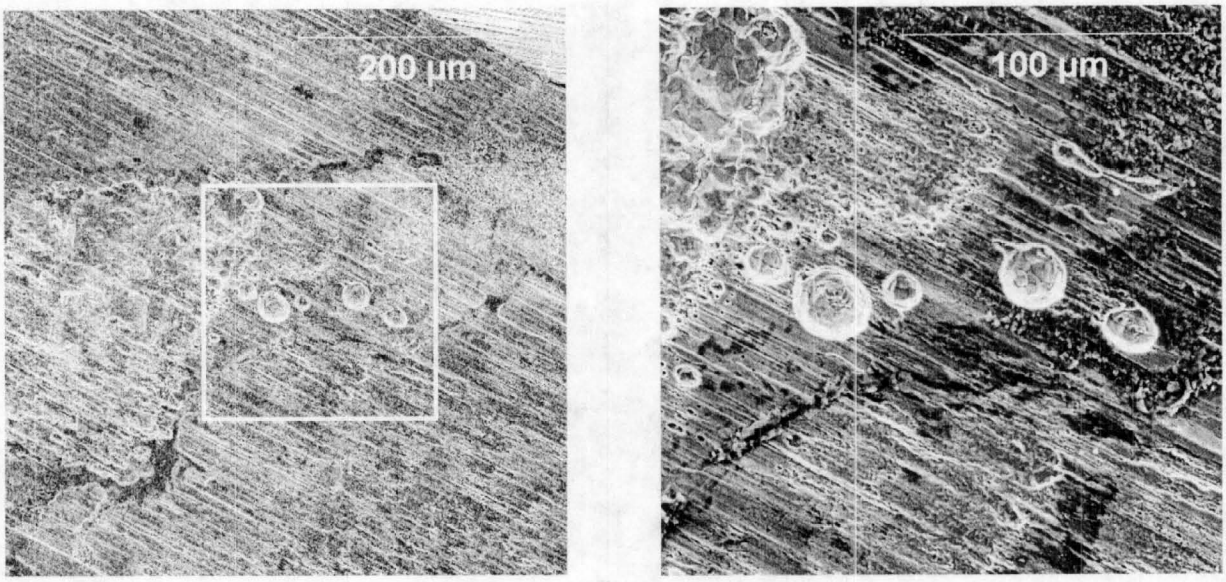

Figure B-11. Medium Magnification SEI (left) SEM image of Sample S03T001560 (Coupon 1B). Area outlined in box is expanded in the SEI image to the right.

Sample S03T001559 (Coupon 1A) showed several patches of corrosion up to several millimeters in size. Figure B-12 is a BEI image of one of these, with a close-up of the lower left corner to

the right. The dark patches are corrosion that was not removed during cleaning. The pit is deeply etched into the coupon and no evidence of the surface striations remaining.

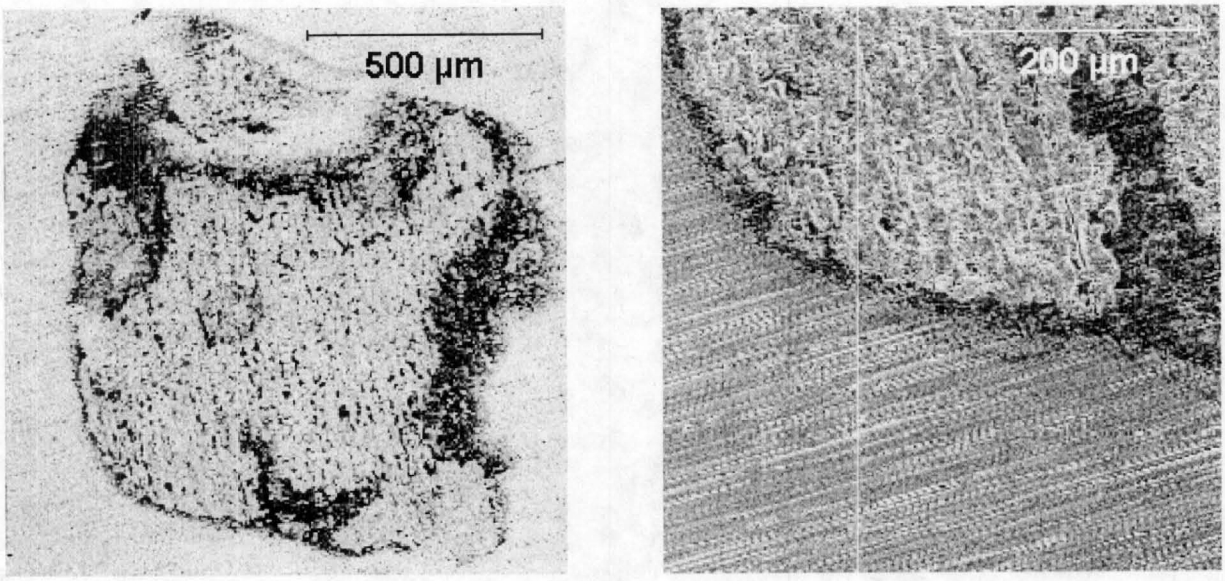

Figure B-12. BEI SEM images of sample S03T001559 (Coupon 1A). Right image is close up of lower left corner of left image.

Other patches of corrosion show a lesser degree of metal attack (Figure B-13). Here, the close up image at the right shows that the striations of the original surface still continue into the corroded patch.

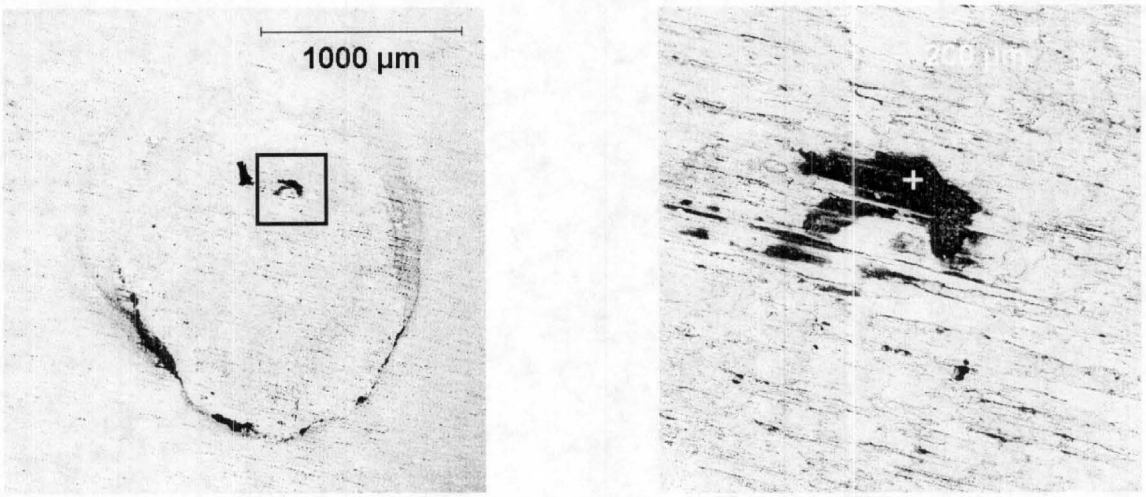

Figure B-13. BEI SEM images of sample S03T001559 (Coupon 1A), shallow pit.

Figure B-14 is an EDS spectrum of the patch of corrosion in the middle of the right image in Figure B-13 (marked with a cross). Note that the corrosion is primarily composed of iron and oxygen with lesser amounts of calcium and silicon.

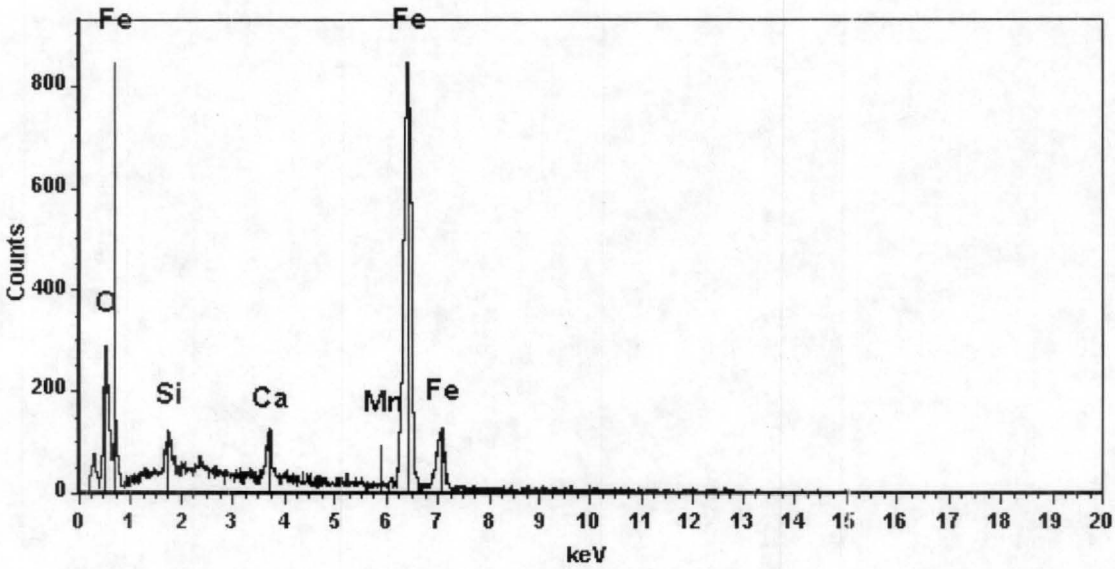

Figure B-14. EDS Spectrum of corrosion from sample S03T001559 (Coupon 1A), shallow pit.

Figure B-15 shows yet another patch on S03T001559 that is heavily corroded. This patch is about 1 millimeter wide and several millimeters long. It is less visible in BEI mode, since the corrosion has been largely cleared away.

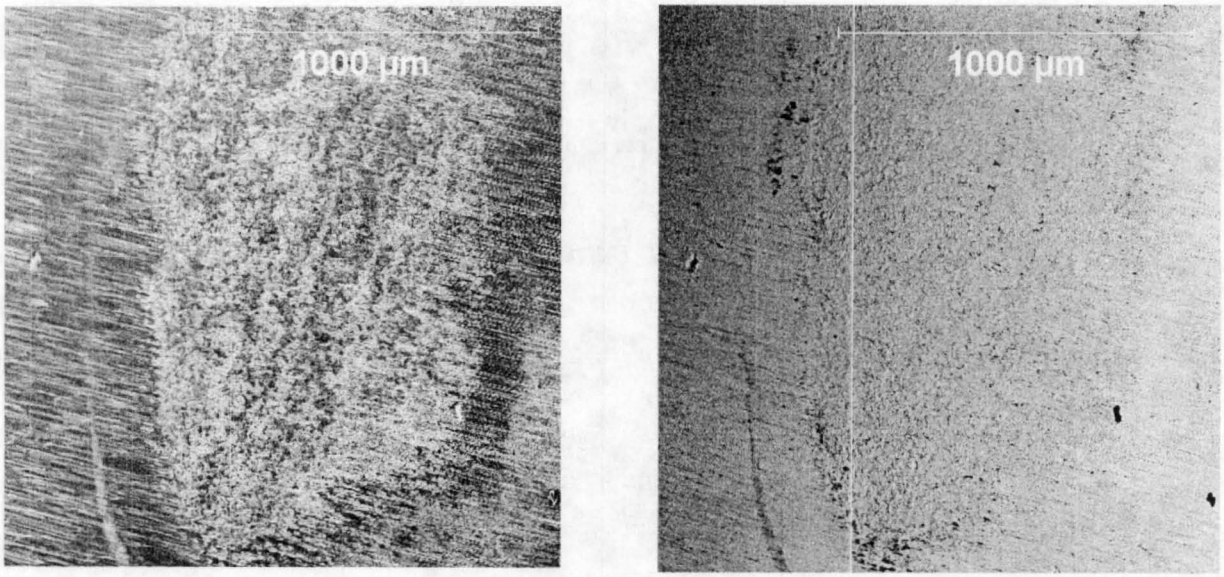

Figure B-15. SEI (left) and BEI (right) SEM images of sample S03T001559 (Coupon 1A), large patch.

Note in the close up of this lower left portion of this patch (Figure B-16) that the corroded area is deeply etched. The etch pattern appears to outline individual metal grains. The metal crystal boundaries are apparently zones of weakness.

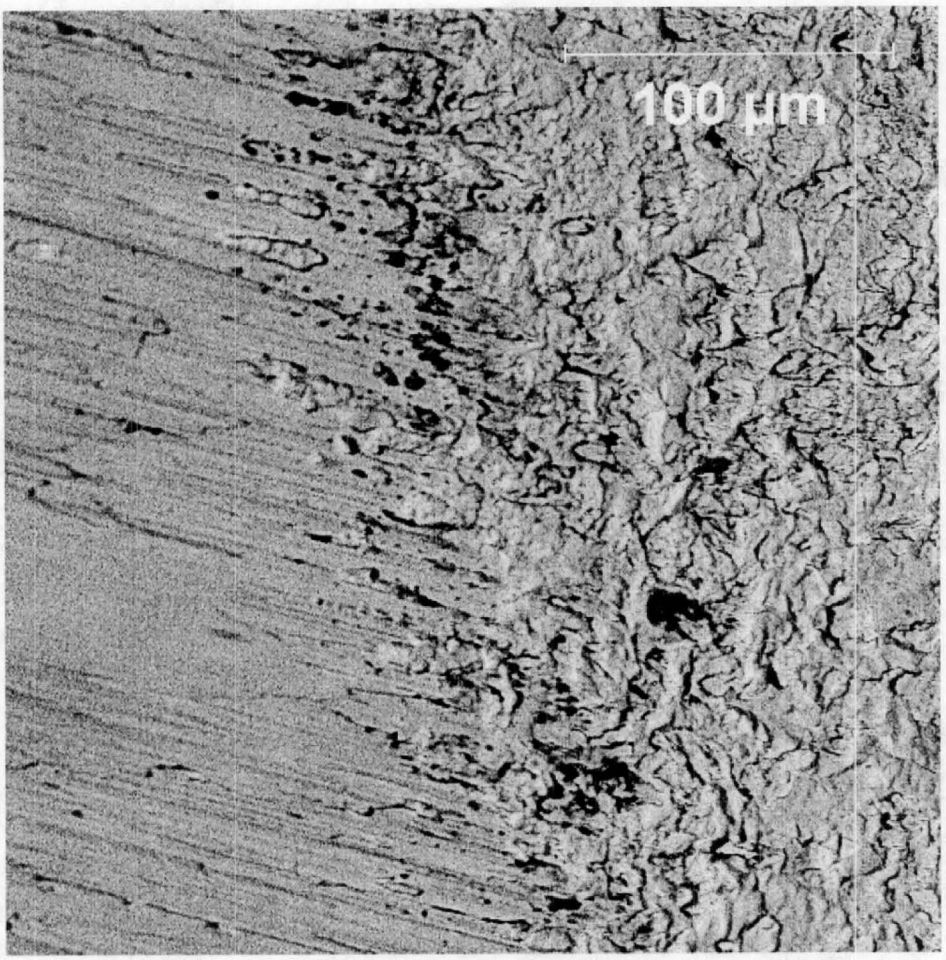

Figure B-16. BEI SEM image of boundary between uncorroded metal (left) and corroded metal (right) on Sample S03T001559 (Coupon 1A).

Summarizing, the Coupons 1M, 2MOH and the Control 515 coupon show no evidence for surface corrosion. Coupons 2A, 3A and 3B have obvious corrosion features that seem to show a progression from mostly etching (3B), to small pitting (2A) to large, deep pits (3A), all in generally small patches. Samples 1A and 1B show evidence for severe corrosion in the form of large patches where the surface features have been completely removed and, in the most severe cases, the individual metal grain boundaries are revealed by the etching. Even on the most severely corroded coupons, large regions of uncorroded surface material remain.

APPENDIX C

CHI SQUARE ALGORITHM FOR TAFEL CORROSION DETERMINATION FROM POWERCORR® CORROSION MEASUREMENT SOFTWARE

The Tafel fit routine carried out an analysis of a data range to perform a nonlinear least-squares fit to the Stern-Geary equation. The equation proposed by Stern-Geary describes a corroding system with two electroactive redox couples:

$$I(\mathrm{E}) = I_{\mathrm{corr}} [10^{(E - E_{corr})/\beta a} - 10^{(E - E_{corr})/\beta c}] \quad \text{(C-1)}$$

In the Stern-Geary equation, I is the net or total current that flows at any one point in time at a specific applied potential, E. I_{corr} is the open-circuit potential for the system. The Tafel proportionally constants for the anodic (oxidation) and cathodic (reduction) are β_a and β_c, respectively.

The Tafel fit routine uses all of the selected data to perform a nonlinear least-squares fit to the Stern-Geary equation, Equation C-1. Both linear and nonlinear least-squares analyses minimize the difference in a calculated result and an observed result as represented by a quantity defined as *chi square*, χ^2. The nonlinear least squares analyses is also sometimes referred to as a χ^2 minimization technique. The formula used for χ^2 in the Tafel fit calculation is:

$$\chi^2 = \{\Sigma [(I_{obs,i} - I_{calc,i}) / s_i]^2\} / (N-4) \quad \text{(C-2)}$$

Where N is the total number of points in the data set, s_i is the standard deviation of the I^{th} current value, $I_{obs,i}$ is the observed current at the i^{th} data point, and $I_{calc,i}$ is the current calculated from the Stern-Geary equation and the corrosion parameters. The $1/(N-4)$ factor normalizes χ^2 allowing a direct comparison of results obtained from data sets of differing sizes.

Inclusion of the standard deviation, s_i, accounts for the variation in the amount of experimental error from data point to data point. In the Tafel fit, s_i, is calculated from the magnitude of the observed current using:

$$s_i = 0.02 \left| I_{obs,i} \right| + 1.0 \times 10^{-9} \quad \text{(C-3)}$$

Equation C-3 weights the points close to E_{corr} more heavily than those further away since $I_{obs,i}$ is always the smallest at E_{corr}. Since a potentiostat must ultimately measure small currents less accurately than large currents, the fixed constant in Equation C-3, 1.0×10^{-9}, limits the diminutive aspects of the standard deviation and the assigning of weights to any single data point.

The use of χ^2 can evaluate the goodness of fit (GOF) of a theoretical curve versus an observed curve for a given set of fit parameters. In this case, the fit parameters are $E(I = 0)$, I_{corr}, β_a *and* β_c.

A final χ^2 value of zero would indicate a perfect fit of the data to the Stern-Geary equation. Higher values indicate poorer fits. Typical values for reasonably good fits will range between 2 and 100. If the results show higher χ^2 values indicate the data are not following the Stean-Geary equation. This manifestation of higher χ^2 values may be the result of:

- attempting to fit data too close to the passive region
- changes in the sample caused by the experiment
- the presence of more than two principal redox reactions in the corroding system.